Low-temperature diffusive transport of electrons in a disordered sandwich structure with quasi-two-dimensional charge transport characteristics

2008 J. Phys.: Condens. Matter 20 425213

(http://iopscience.iop.org/0953-8984/20/42/425213)

IOP PUBLISHING JOURNAL OF PHYSICS: CONDENSED MATTER

J. Phys.: Condens. Matter **20** (2008) 425213 (16pp) doi:10.1088/0953-8984/20/42/425213

Low-temperature diffusive transport of electrons in a disordered sandwich structure with quasi-two-dimensional charge transport characteristics

Huan-Sheng Wei[1], **Li Chang**[1] **and George Y Wu**[1,2,3]

[1] Department of Physics, National Tsing-Hua University, Hsin-Chu, Taiwan, 300, Republic of China

[2] Department of Electrical Engineering, National Tsing-Hua University, Hsin-Chu, Taiwan, 300, Republic of China

E-mail: yswu@ee.nthu.edu.tw

Received 31 January 2008, in final form 17 August 2008
Published 25 September 2008
Online at stacks.iop.org/JPhysCM/20/425213

Abstract

We present the theoretical study of weak localization in a disordered sandwich structure, which consists of a thin, dirty metallic film bounded by nearly insulating materials with electrical current primarily located in the metallic film. The conductance correction, $\delta G(B)$, due to backscattering interference is calculated within the weak-localization theory as a function of perpendicular magnetic field B. It is found that, for a certain range of structural/material parameters, both the conductance correction $\delta G(B = 0)$ and magnetoconductance (MC) show a weak temperature dependence (i.e. saturation) over a range of low temperatures, as opposed to those of a freestanding metallic film, which show a strong temperature dependence. At further lowered temperatures, it shows that $\delta G(B = 0)$ and MC may or may not diverge, depending on the structure. If the structure is thin like a film, $\delta G(B = 0)$ and MC both eventually diverge. On the other hand, if the structure is thick like a bulk, saturation of $\delta G(B = 0)$ persists to 0 K but MC is likely to diverge. We also fit the calculated MC of sandwich structures with the weak-localization theory suitable for a freestanding film, with the phase breaking time τ_φ in the theory being the fitting parameter. This gives a nominal phase breaking time $\tau_\varphi^{(\mathrm{eff})}$, which is nearly constant over a range of low temperatures. The implication of the work is discussed in connection with the issue of dephasing time saturation. The limitation of the present theory is examined and directions for future extension are suggested.

(Some figures in this article are in colour only in the electronic version)

1. Introduction

The physics of diffusive transport in disordered systems constitutes a fascinating field in condensed matter physics. An important work to unveil the physics of disordered systems is the renormalization group-theoretical analysis, by Abraham *et al*, of non-interacting, low-dimensional cases [1]. In essence, it leads to the phenomenal conclusion that disordered systems are insulators in one dimension (1D) and two dimensions (2D). The conclusion is supported by the theory of weak localization, which calculates δR, the correction to classical resistance due to the quantum interference occurring between a backscattering path and its time-reversal counterpart [2]. It shows that δR diverges in low-dimensional systems. Moreover, it shows that the divergence of δR also occurs in homogeneous, quasi-low-dimensional systems, where the motion of electrons perpendicular to the system is either diffusive or just quantum mechanical, and confined by abrupt, reflecting boundaries.

[3] Address for correspondence: Department of Electrical Engineering, National Tsing-Hua University, Hsin-Chu, Taiwan, 300, Republic of China.

An important timescale for the backscattering interference is the so-called phase breaking (or dephasing) time, τ_φ. In non-magnetic systems, it is determined by the inelastic scattering, for example, between electrons or between electrons and phonons. Such scattering brings randomness into the phase of quantum amplitude, thus breaking phase coherence and setting the timescale for interference (which occurs within the length of time when the phases are coherent). In general, τ_φ increases with decreasing temperature. Specifically, it becomes infinite at 0 K [3], resulting in divergent δR for low-dimensional systems.

On the other hand, apart from inelastic scattering, the interference can also be suppressed by a magnetic field. With the field, the time-reversal symmetry is broken and the quantum amplitudes of backscattering paths in a time-reversal pair are no longer in phase. The interference is thereby reduced, causing a change in conductance/resistance, called magnetoconductance (MC)/magnetoresistance (MR). Almost since the early study of weak-localization phenomena, the MC/MR measurement has become an important tool for the investigation of weakly disordered systems, and most of the experiments have confirmed the theory of weak localization [4]. The primary exceptions come from the recent work of Mohanty and Webb with one-dimensional wires [5], and the earlier data (some of which being for quasi-two-dimensional systems) taken by other groups [6] (with the latter being also analyzed in [5]). In summary, a saturated MC has been found at low temperatures, and the finding has been interpreted as suggesting the existence of intrinsic phase decoherence at 0 K. Such a decoherence has the non-trivial implication for diffusive transport at 0 K—although inelastic scattering vanishes, the decoherence still imposes an upper bound on τ_φ. Consequently, this limits the divergence of δR and contradicts the current belief (e.g. [1]) mentioned earlier that electrons are localized in disordered low-dimensional systems. In order to resolve the contradiction, Pierre and Birge have performed a similar measurement and argued that the observed saturation can be attributed to dilute magnetic impurities [7]. But Huang *et al* demonstrate otherwise in a recent experiment, where a sharp upturn in the MC curve is observed at the end of saturation and which cannot be explained in terms of magnetic impurity scattering [8]. In the mean time, theoretical explanations based on the idea of intrinsic dephasing have appeared. In particular, Golubev and Zaikin have examined the zero-point fluctuation-induced decoherence [9] and Zawadowski *et al* have looked into the dephasing with two-level defects [10]. On the other hand, Marquardt *et al* have recently provided a comprehensive theoretical analysis showing that the Pauli exclusion principle suppresses the quantum fluctuation of the environment for electrons near the Fermi level [11]. This work clarifies the role of zero-point fluctuation and leads to the conclusion of infinite τ_φ at 0 K, in agreement with the earlier theoretical work in [3]. Meanwhile, routes other than the intrinsic mechanism have been pursued. For example, Germanenko *et al* have studied a model where the system is two-dimensional and has a multiply connected topology, with electrons diffusing in percolating, constricted channels [12]. As a result of the topology, the magnetoresistance (MC) is saturated according to their numerical simulation.

In this work, we do not attempt to prove/disprove the existence of intrinsic phase breaking or, equivalently, electron localization in low-dimensional systems. Instead, we approach from a different direction and examine a closely connected problem—the possibility of δR or MC being saturated over a range of temperatures for a quasi-two-dimensional (Q2D) system, within the weak-localization theory. In particular, we study the possibility of the saturation as a consequence of the inhomogeneity in a structure. The idea is summarized as follows. We begin with writing the overall resistance R as a functional of the local conductivity $\sigma(\vec{r})$, i.e. $R = R[\sigma(\vec{r})]$. This gives the quantum correction to R as the integral

$$\delta R = \int \mathrm{d}\vec{r} \frac{\delta R}{\delta \sigma} \delta\sigma(\vec{r}), \tag{1.1}$$

where $\delta\sigma(\vec{r})$ is the quantum correction to $\sigma(\vec{r})$. In the theory of weak localization, one has, roughly,

$$\delta\sigma(\vec{r}) \propto \sum_\beta \frac{|\Psi_\beta(\vec{r})|^2}{\lambda_\beta + 1/\tau_\varphi}, \tag{1.2}$$

with λ_βs and ψ_βs in (1.2) being the eigenvalues and eigenfunctions satisfying a diffusion-type eigenequation. Notably, the equation has the characteristic property of always having $\lambda_\beta = 0$ as a solution. Correspondingly, there is a singular term in the sum in (1.2), which dominates and, in particular, diverges with a simple pole, in the limit where $\tau_\varphi \to \infty$ (which happens at vanishing temperature, as mentioned earlier). This special pole is called the diffusion pole, and is the main reason for the divergence of $\delta\sigma(\vec{r})$ in low-dimensional systems. However, it is worthwhile noting that, in general, a sum containing a singular term does not necessarily blow up. For example, in the case of a three-dimensional system, the eigenvalues may be continuous and the summation in (1.2) performed over the corresponding continuous spectrum may very well be finite. Below, we shall focus on Q2D systems and discuss an alternative, interesting scenario where the divergence of $\delta\sigma(\vec{r})$ may be suppressed (but does not disappear). We begin with noting that all the terms in (1.2), including the singular one with a pole, are each weighted by a corresponding numerator $|\Psi_\beta(\vec{r})|^2$. The weight factor may actually play an important role in determining the magnitude of a term. For example, a nearly vanishing $|\Psi_\beta(\vec{r})|^2$ for the singular term could well suppress the singularity and, hence, the divergence of $\delta\sigma(\vec{r})$ as well. In the case of an ideal Q2D system (which we take to be a homogeneous, freestanding film), such suppression does not occur, as explained in the following. We estimate $|\Psi_\beta(\vec{r})|^2$ first. Because of the homogeneity, we have $O(|\Psi_\beta(\vec{r})|^2) \sim 1/twl$, irrespective of β, where t = thickness, w = width and l = length of the film. Thus, the weight factors are all of the same order and unable to differentiate the magnitude of various terms. It follows, in the case of a homogeneous system, that the relative magnitude of each term in (1.2) can only depend on the corresponding denominator $\lambda_\beta + 1/\tau_\varphi$. As having been explained earlier in terms of the diffusion

pole, this denominator dependence results in the likelihood of dominance by the singular term in (1.2) and the divergence of $\delta\sigma(\vec{r})$ as well. On the other hand, a different situation can arise if the system is inhomogeneous. In particular, if it is drastically modulated, $|\Psi_\beta(\vec{r})|^2$s would be rapidly varying in space and, for some βs, might be nearly vanishing in the region of importance (to the integral of δR in (1.1)) where the derivative $\delta R/\delta\sigma$ is large. Correspondingly, some of the terms in (1.2) would be suppressed in their contribution to δR and the upshot is that, if the singular term happens to be among them, δR may appear to show a non-divergent (or weakly temperature-dependent) behavior over a range of low temperatures.

Following the above discussion, we examine the Q2D systems which are spatially modulated. The Q2D structure is defined, in this work, as a system which has classical current limited mainly within a thin layer. In particular, the structure considered is a sandwich type and consists of a thin, dirty metallic film (called the H layer) bounded by nearly insulating layers (called L layers). The electric current, as shown later, is confined mainly in the H layer. In general, the sandwich structure can be classified in the following way according to its various length scales. Let H = H-layer thickness, L = L-layer thickness, $l_{\rm H}$ = elastic mean free path in the H layer, $l_{\rm L}$ = elastic mean free path in the L layer, $\lambda_{\rm H}$ = electron wavelength in the H layer and $\lambda_{\rm L}$ = electron wavelength in the L layer. The theoretical derivation in the present work considers only the diffusive structures, where $H > l_{\rm H} > \lambda_{\rm H}$ and $L > l_{\rm L} > \lambda_{\rm L}$ are both satisfied. We call these the diffusion-confined structures. On the other hand, there are systems with $H < \lambda_{\rm H}$, or $L < \lambda_{\rm L}$, or electron wavefunctions decaying in L layers, for example. Such systems are all called quantum-confined ones and, rigorously speaking, are not covered by the present theoretical derivation. Among these are some systems which may also be relevant to current dephasing experiments. Nonetheless, our study focuses on the diffusion-confined sandwich structure for the following reasons. First of all, as shall be discussed in section 2, such a structure may simulate some of the experimental systems used for the study of 2D weak localization Second, as shall be discussed later, although the current in the structure is primarily confined in the metallic film, the structure shows an interesting behavior distinct from that of an isolated film, namely, suppression of both conductance correction and magnetoconductance. Third, in the case of diffusion-confined structures, diffusive transport theory is valid and thus the weak-localization phenomenon is susceptible to a clean-cut analysis with diffusive transport theory. Results of such an analysis may also be used as a guide for the future study of varied structures such as quantum-confined ones. Given the above reasons, we are thus motivated to study a diffusion-confined sandwich structure.

The mathematics of our work focuses on deriving the theory of weak localization appropriate for such a structure. The work uses the isolated film as a reference and compares the sandwich structure with the film, in order to demonstrate the suppression of weak localization in the sandwich relative to that in the film. It shows that, if one inadvertently uses the film theory to interpret the sandwich data, the 'effective dephasing time' would appear suppressed/saturated. Furthermore, in the absence of a rigorous derivation for quantum-confined systems, the theory is used as a guide to discuss dephasing experiments, where quantum-confined systems are as likely to be involved as diffusion-confined ones. In particular, this work carries out the calculation of δG (with $\delta G \equiv -\delta R/R^2$ being the quantum correction to conductance) and MC both as functions of $1/\tau_\varphi$ for the sandwich structure. We regard $1/\tau_\varphi$ as due to inelastic scattering and hence a monotonically increasing function of temperature. Specifically $1/\tau_\varphi = 0$ at 0 K. The main result of the work shows that, for a certain range of structural/material parameters, the sandwich structure may show properties different from those of homogeneous Q2D systems, namely its δG/MC are saturated over a range of low $1/\tau_\varphi$ (or low temperatures). At further lowered temperatures, it shows that δG/MC may or may not diverge, depending on the structure. If the aspect ratio *thickness*: *length* $\ll 1$, meaning that the structure is film-like, then δG/MC eventually diverges. On the other hand, if *thickness*: *length* $\sim O(1)$, meaning that the structure is bulk-like, saturation of δG persists to 0 K but MC is likely to diverge. We may as well stress that there is no conflict between our result for the sandwich structure and the localization argument of the Gang of Four (in [1]) for a real 2D or an ideal Q2D system since the structures are different. With the latter, the system is homogeneous, electrons are well confined in the perpendicular direction, and δG/MC are temperature-sensitive at low temperatures. We also fit the calculated MC of the sandwich structure with the orthodox weak-localization theory of an (ideal) freestanding film, with τ_φ of the film theory being the fitting parameter. This gives a nominal phase breaking time $\tau_\varphi^{(\rm eff)}$ which is nearly constant over a range of low temperatures.

The presentation is organized as follows. In section 2, we describe details of the sandwich structure and its connection to experimental systems. In section 3, we describe the calculation of backscattering interference for the structure. In section 4, we discuss qualitatively the overall low-temperature behavior of δG and MC. In particular, we estimate the characteristic $1/\tau_\varphi$ where δG/MC begins to saturate. We also discuss the upturn of δG/MC with a film-like structure at extremely low temperatures and the zero-temperature saturation of δG/MC with a bulk-like structure. Moreover, we provide quantitative expressions within perturbation theory for the calculation of δG and MC. In section 5, we derive analytical estimates within logarithmic accuracy for δG/MC as functions of $1/\tau_\varphi$. In section 6, we carry out numerical calculations and compare the result obtained for a film-like sandwich structure with that for a freestanding metallic film. We fit the calculated MC of the sandwich structure with the weak-localization theory of a freestanding film and show the behavior of $\tau_\varphi^{(\rm eff)}$ at low temperatures. In section 7, we remark on the theory, summarize and conclude the study. A simple physical picture for dephasing is offered in terms of electron lifetime in the H layer. A brief analysis, guided by the present theory, is given of dephasing experiments, where a theoretical estimate of saturated dephasing time is compared with the experimental value. Limitations and any future extension of the present theory are discussed.

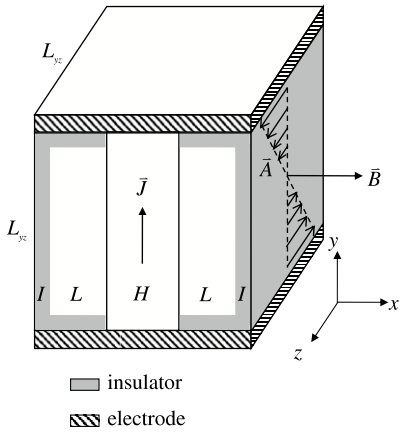

Figure 1. The L–H–L sandwich structure. The middle region is the dirty metallic film called the H region, and on both sides of it are nearly insulating L regions. The structure is capped with perfectly insulating I slabs. The electrodes are attached only to the H layer and isolated from the L regions by thin layers of insulator.
H = thickness of the H layer and L = thickness of the L layer. The lengths of the structure in y and z directions are both L_{yz}. The applied magnetic field is perpendicular to the layer, i.e. $\vec{B} = (B, 0, 0)$, with a vector potential $\vec{A} = (0, 0, By)$.

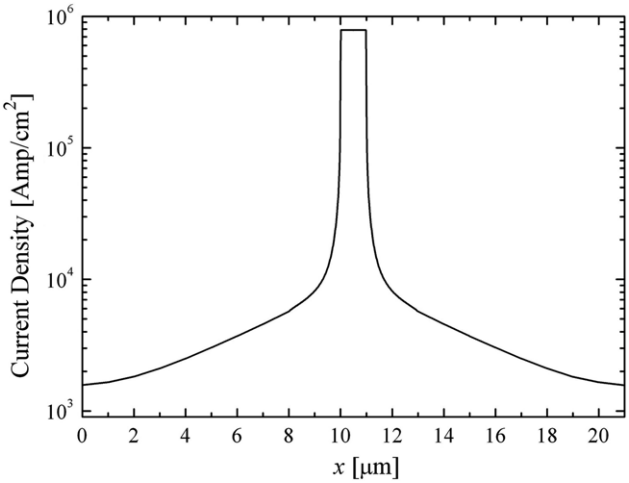

Figure 2. The current density simulated with MEDICI for a semiconductor sandwich structure. DC bias $V = 5$ V is applied and the current density at $y = 5$ μm is plotted. The structure is characterized by the widths $H = 1$ μm, $L = 10$ μm, the electron densities $n_{\rm H} = 10^{20}$ cm^{-3}, $n_{\rm L} = 10^{14}$ cm^{-3}, the mobilities $\mu_{\rm H} = 10$ cm^2 V^{-1} s^{-1}, $\mu_{\rm L} = 10^5$ cm^2 V^{-1} s^{-1}, and the conductivities $\sigma_{\rm H} = 160$ A cm^{-1} V^{-1}, $\sigma_{\rm L} = 1.6$ A cm^{-1} V^{-1}, at the temperature 300 K.

2. Model structure and its connection to experimental systems

The system considered is an L–H–L layered structure immersed in a magnetic field perpendicular to the layers, as shown in figure 1. In the middle is the H layer, a thin, dirty metallic region, highly conductive and bounded by nearly insulating L layers, with L and H being the thicknesses of L and H layers, respectively. We take each layer to be a square film, with L_{yz} being the side length of the square. Moreover, we take $L_{yz} \gg H$ so the H layer is indeed a thin film. The L–H–L structure is the electrically active part of the system, and is capped on both sides by I slabs, which are perfectly insulating materials. The electrodes are attached only to the H layer.

Two classes of sandwich structures are considered in this work. If the L layer is thin enough such that the total thickness of L–H–L obeys $H + 2L : L_{yz} \ll 1$, we have a film-like structure. On the other hand, if the aspect ratio $L : L_{yz} \sim O(1)$, we call it a bulk-like structure.

The L–H–L sandwich structure is quantitatively characterized by the parameters α, β, γ and χ, defined by the following expressions, namely, $L = \chi H$, $l_{\rm L} = L/\gamma$ and $l_{\rm H} = H/\alpha$ where $l_{\rm L}$ and $l_{\rm H}$ are the elastic mean free paths of electrons in the two regions, and $v_{\rm H}/v_{\rm L} = \beta l_{\rm L}/l_{\rm H}$, where $v_{\rm L}$ and $v_{\rm H}$ are the electron Fermi velocities. It follows that $D_{\rm H}/D_{\rm L} = \beta$ where $D_{\rm H}$ and $D_{\rm L}$ are diffusivities, $\sigma_{\rm H}/\sigma_{\rm L} = \alpha\beta^2\chi/\gamma$ where $\sigma_{\rm H}$ and $\sigma_{\rm L}$ are classical electrical conductivities, and $G_{\rm H}/G_{\rm L} = \alpha\beta^2/\gamma$ where $G_{\rm H}$ and $G_{\rm L}$ are classical conductances. Therefore, α, β, γ and χ can be used to control the contrast of transport properties between the H and L regions.

Figure 2 shows the profile of current density obtained by a calculation with the device simulation software MEDICI [13] for a sandwich structure with $G_{\rm H}/G_{\rm L} \sim 10$, which simulates closely the typical system considered in this work, except that it is a semiconductor. Specifically, the device is characterized by the thicknesses $H = 1$ μm, $L = 10$ μm, the electron densities $n_{\rm H} = 10^{20}$ cm^{-3}, $n_{\rm L} = 10^{14}$ cm^{-3}, the mobilities $\mu_{\rm H} = 10$ cm^2 V^{-1} s^{-1}, $\mu_{\rm L} = 10^5$ cm^2 V^{-1} s^{-1}, and the conductivities $\sigma_{\rm H} = 160$ A cm^{-1} V^{-1}, $\sigma_{\rm L} = 1.6$ A cm^{-1} V^{-1}, at the temperature 300 K. The profile in figure 2 shows that the current density is primarily distributed in the thin H layer. Integrating the current density in figure 2, we find the current ratio $I_{\rm H}/I_{\rm L} \sim G_{\rm H}/G_{\rm L} \sim 10 \gg 1$ at $y = 5$ μm, halfway between the top and bottom electrodes, where $I_{\rm H}$ and $I_{\rm L}$ are the currents flowing in the H and L regions, respectively. This confirms the thin H layer as the main conducting channel, while it also shows a small fraction ($\sim O(G_{\rm L}/G_{\rm H})$) of total current flowing in the L layer, despite this layer not being directly attached to the electrodes.

Throughout the rest of this presentation, we take $\alpha, \gamma > 1$ such that $L > l_{\rm L}$ and $H > l_{\rm H}$. This justifies our following treatment of transport in the structure with the theory of diffusive transport (including backscattering correction). Moreover, we take the various contrasts to satisfy the following inequalities, namely $v_{\rm H}/v_{\rm L}[=\alpha\beta\chi/\gamma] \gg 1$, $D_{\rm H}/D_{\rm L}[=\beta] \geqslant O(1)$, $\sigma_{\rm H}/\sigma_{\rm L}[=\alpha\beta^2\chi/\gamma] \gg 1$ and $G_{\rm H}/G_{\rm L}[=\alpha\beta^2/\gamma] \gg 1$. The foregoing contrast inequalities can be satisfied by the choice of a sufficiently large β, χ or α/γ. In the following, we use specifically the set of parameters

$$\beta \gg 1, \qquad \alpha, \gamma > 1, \qquad \alpha/\gamma > 1, \qquad \chi \geqslant O(1)$$

(for film-like structures)

or alternatively

$$\beta \geqslant O(1), \qquad \alpha, \gamma > 1, \qquad \alpha/\gamma > 1, \qquad \chi \gg 1$$

(for bulk-like structures).

Both sets greatly simplify the analysis. The contrast inequalities are satisfied by either choice of parameters, and

when the inequalities do hold, both the electron population and the electrical current are primarily concentrated in the thin H layer. A structure with such a feature of confinement seems to be among the reasonable models for experimental Q2D systems. Moreover, with the condition $H > l_{\mathrm{H}}$ and $L > l_{\mathrm{L}}$, our structure describes diffusion-confined systems.

It is important to note that, apart from the H layer and I slab, our model also includes the lowly conductive L region in the structure, to simulate the physical/chemical transition from the highly conductive H layer into the insulating I slab. Inclusion of the L region gives a more complete account of a general Q2D system. In the case of a film-like structure, both the (electrically active) H and L regions are thin layers, and the structure models an experimental Q2D system well insulated (by I slabs) from the surroundings. On the other hand, for a bulk-like structure, we have $L : L_{yz} \sim O(1)$. With a wide L region also being electrically active (apart from the highly conductive H layer), the bulk-like structure models an experimental Q2D system which is not perfectly insulated from the surroundings.

Last, we note that an actual non-freestanding film (i.e. metal film on an insulating substrate) may best be modeled by an asymmetric I–L–H sandwich structure, with I being the substrate, H the film and L the I–H interface. However, the calculation below considers a symmetric (I–L–H–L–I) structure so that the reflection symmetry of the system may be used to simplify the mathematical analysis. The derived results also hold qualitatively for asymmetric systems.

3. Backscattering Cooperon

Next, we discuss the backscattering Cooperon $C(\vec{r},\vec{r})$, which determines the quantum correction $\delta\sigma$ to the classical conductivity through the following expression [2]:

$$\delta\sigma(\vec{r}) = -G_0 \cdot D\tau C(\vec{r},\vec{r}) \qquad (G_0 \equiv 2e^2/\pi\hbar).$$

$C(\vec{r},\vec{r})$ satisfies, in the absence of a magnetic field, the diffusion-type equation for the modulated structure considered [14]:

$$\left(-\frac{1}{d}\nabla l(x)\nabla v(x) + \frac{1}{\tau_\varphi(x)}\right) C(\vec{r},\vec{r}') = \frac{1}{\tau(x)}\delta(\vec{r}-\vec{r}') \tag{3.1}$$

with d = dimensionality, $l(x)$ = mean free path, $v(x)$ = Fermi velocity, $\tau_\varphi(x)$ = phase breaking time and $\tau(x)$ = mean free time. The x direction is taken to be perpendicular to the structure. In the presence of a magnetic field B, we replace $\vec{\nabla}$ with $\vec{\nabla} - \frac{2ie}{\hbar c}\vec{A}(\vec{r})$ where $\vec{A}$ is the vector potential. $C(\vec{r},\vec{r})$ in equation (3.1) is a Green function and so can be expressed as

$$C(\vec{r},\vec{r}) = \sum_\beta \frac{|\Psi'_\beta(\vec{r})|^2 v(x)/\tau(x)}{\lambda'_\beta} \tag{3.2}$$

with λ'_β and Ψ'_β satisfying the auxiliary equation

$$\left[-\frac{1}{d}\frac{\partial}{\partial x}l(x)\frac{\partial}{\partial x}v(x) - D(x)\frac{\partial^2}{\partial y^2} + D(x)\left(\frac{1}{\mathrm{i}}\frac{\partial}{\partial z} - \frac{2eB}{\hbar c}y\right)^2 + \frac{1}{\tau_\varphi(x)}\right]\Psi'_\beta(\vec{r}) = \lambda'_\beta\Psi'_\beta(\vec{r}) \tag{3.3}$$

where $D(x)$ = diffusivity and the gauge $\vec{A}(\vec{r}) = (0, 0, By)$ has been chosen for the vector potential. Let $\beta = (n, \mu)$. Equation (3.3) can be satisfied with

$$\mu = k_\parallel$$

$$\Psi'_{n,\mu}(\vec{r}) = \psi'_{n,k_\parallel}(x)\,\mathrm{e}^{\mathrm{i}\vec{k}_\parallel\cdot\vec{r}_\parallel}/L_{yz}$$

for $B = 0$, where $\vec{k}_\parallel = (k_y, k_z)$ and $\vec{r}_\parallel = (y, z)$, and with

$$\mu = m = \text{integer}$$

$$\Psi'_{n,\mu}(\vec{r}) = \psi'_{n,m}(x)u_m\left(y - \frac{\hbar c}{2eB}k_z\right)\mathrm{e}^{\mathrm{i}k_z z}/\sqrt{L_{yz}}$$

for $B \neq 0$ where u_m = asimple harmonic oscillator wavefunction. Now, $\lambda'_{n,\mu}$ and $\psi'_{n,\mu}$ satisfy

$$\left(-\frac{1}{d}\frac{\partial}{\partial x}l(x)\frac{\partial}{\partial x}v(x) + D(x)K_\mu^2 + \frac{1}{\tau_\varphi(x)}\right)\psi'_{n,\mu}(x) = \lambda_{n,\mu}(B)'\psi'_{n,\mu}(x)$$

where

$$K_\mu^2 = \begin{cases} k_y^2 + k_z^2, & \text{for } B = 0 \\ \left(m + \dfrac{1}{2}\right)\dfrac{4eB}{\hbar c}, & \text{for } B \neq 0. \end{cases}$$

We treat $\frac{1}{\tau_\varphi(x)}$ in the above equation perturbatively and replace the equation with the unperturbed equation

$$\left(-\frac{1}{d}\frac{\partial}{\partial x}l(x)\frac{\partial}{\partial x}v(x) + D(x)K_\mu^2\right)\psi_{n,\mu}(x) = \lambda_{n,\mu}(B)\psi_{n,\mu}(x) \tag{3.4}$$

where

$$\psi_{n,\mu} \approx \psi'_{n,\mu},$$
$$\lambda_{n,\mu}(B) \approx \lambda_{n,\mu}(B)' - \left\langle n,\mu\left|\frac{1}{\tau_\varphi(x)}\right|n,\mu\right\rangle. \tag{3.4$'$}$$

Equation (3.4) simulates the quantum mechanics of a particle moving in a one-dimensional potential $D(x)K_\mu^2$. This is the main equation to be solved in this work. The solution is required to obey the boundary condition that

$$v(x)\psi_{n,\mu}(x) \qquad \text{and} \qquad l(x)\frac{\partial}{\partial x}[v(x)\psi_{n,\mu}(x)]$$

is continuous at the H/L interface. At the L/I interface, we impose $\frac{\partial}{\partial x}\psi_{n,\mu}(x) = 0$, meaning vanishing normal current there. Normalization of the solution requires $\int \mathrm{d}x|\psi_{n,\mu}(x)|^2 v(x) = 1$.

For (un-normalized) even-parity solutions at $x > 0$ (with the origin $x = 0$ chosen to be at the vertical plane of reflection symmetry of the structure), we have

$$\psi_{n,\mu}(x) = \begin{cases} \cos(\gamma_{n,\mu}^{(\mathrm{H})}x) & \text{in H-region} \\ C_{n,\mu}\cos[\gamma_{n,\mu}^{(\mathrm{L})}(x - H/2 - L)] & \text{in L-region} \end{cases}$$
$$-l_{\mathrm{H}}\gamma_{n,\mu}^{(\mathrm{H})}\tan(\gamma_{n,\mu}^{(\mathrm{H})}H/2) = l_{\mathrm{L}}\gamma_{n,\mu}^{(\mathrm{L})}\tan(\gamma_{n,\mu}^{(\mathrm{L})}L) \tag{3.5a}$$

where $\gamma_{n,\mu}^{(i)} = (\lambda_{n,\mu}/D_i - K_\mu^2)^{1/2}$, i = H, L and $C_{n,\mu}$ is a constant, and the last transcendental equation determines the eigenvalues of even-parity solutions. For solutions of odd parity at $x > 0$

$$\psi_{n,\mu}(x) = \begin{cases} \sin(\gamma_{n,\mu}^{(\mathrm{H})} x) & \text{in H-region} \\ C_{n,\mu} \cos[\gamma_{n,\mu}^{(\mathrm{L})}(x - H/2 - L)] & \text{in L-region} \end{cases}$$

$$l_{\mathrm{H}} \gamma_{n,\mu}^{(\mathrm{H})} \cot(\gamma_{n,\mu}^{(\mathrm{H})} H/2) = l_{\mathrm{L}} \gamma_{n,\mu}^{(\mathrm{L})} \tan(\gamma_{n,\mu}^{(\mathrm{L})} L). \tag{3.5b}$$

Analysis of the transcendental equations in (3.5*a*) and (3.5*b*) leads to the conclusion that the solutions are standing waves of two types. The first type is termed an H state, having a wavevector $\gamma_{n,\mu}^{(\mathrm{H})} \sim n_{\mathrm{H}}\pi/H$ thus behaving as a standing wave in the H region. The second type is termed an L state, with a wavevector $\gamma_{n,\mu}^{(\mathrm{L})} \sim n_{\mathrm{L}}\pi/L$ thus behaving like a standing wave in the L region. The eigenvalue spectrum has the following structure, namely a dense set of L states, with narrow level spacing of $O(D_{\mathrm{L}}/L^2)$, mixing with a dilute set of H states, the latter having wide level spacing $O(D_{\mathrm{H}}/H^2)$. Moreover, analysis of equations (3.5*a*) and (3.5*b*) for $\psi_{n,\mu}$ also shows that an L state generally has a distribution primarily located in the L region, with the integrated 'probability' for the region

$$p_{n,\mu}|_{\mathrm{L}} \equiv \int \mathrm{d}x_{\mathrm{L}} \, |\psi_{n,\mu}(x_{\mathrm{L}})|^2 v(x_{\mathrm{L}}) = 1 - O(\gamma/\alpha\beta\chi^2), \tag{3.6a}$$

being close to unity, while its integrated probability over the H region

$$p_{n,\mu}|_{\mathrm{H}} \equiv \int \mathrm{d}x_{\mathrm{H}} \, |\psi_{n,\mu}(x_{\mathrm{H}})|^2 v(x_{\mathrm{H}}) = O(\gamma/\alpha\beta\chi^2), \tag{3.6b}$$

is near zero. In contrast, an H state has a substantial probability in the H layer, with

$$p_{n,\mu}|_{\mathrm{H}} \geqslant 1 - O(\gamma/\alpha), \tag{3.6c}$$

while

$$p_{n,\mu}|_{\mathrm{L}} \leqslant O(\gamma/\alpha). \tag{3.6d}$$

Variation of $p_{n,\mu}|_{\mathrm{H}}$ with states is shown in figure 3. The peaks belong to H states and $p_{n,\mu}|_{\mathrm{H}}$ drops drastically for L states. The contrast between H states and L states becomes strong with increasing α/γ, β and χ.

In terms of $p_{n,\mu}|_{\mathrm{H}}$ and $p_{n,\mu}|_{\mathrm{L}}$, we can re-express equation (3.4′) as

$$\lambda_{n,\mu}(B)' \approx \lambda_{n,\mu}(B) + \frac{1}{\tau_\varphi^{(n,\mu)}}$$

where $\frac{1}{\tau_\varphi^{(n,\mu)}} \equiv \frac{p_{n,\mu}|_{\mathrm{H}}}{\tau_\varphi(x)|_{x\in H}} + \frac{p_{n,\mu}|_{\mathrm{L}}}{\tau_\varphi(x)|_{x\in L}}$. Moreover, we make the approximation that $\frac{1}{\tau_\varphi^{(n,\mu)}} \sim \frac{1}{\tau_\varphi^{(\mathrm{H})}}$ for H states and $\frac{1}{\tau_\varphi^{(n,\mu)}} \sim \frac{1}{\tau_\varphi^{(\mathrm{L})}}$ for L states, both of which are independent of (n, μ). $\frac{1}{\tau_\varphi^{(\mathrm{H})}}$ and $\frac{1}{\tau_\varphi^{(\mathrm{L})}}$ represent typical expectation values $< n, \mu|\frac{1}{\tau_\varphi(x)}|n, \mu >$ for H and L states, respectively. The approximation here neglects the variation of $\langle n, \mu|\frac{1}{\tau_\varphi(x)}|n, \mu\rangle$ with (n, μ) and simplifies the calculation of $C(\vec{r}, \vec{r})$.

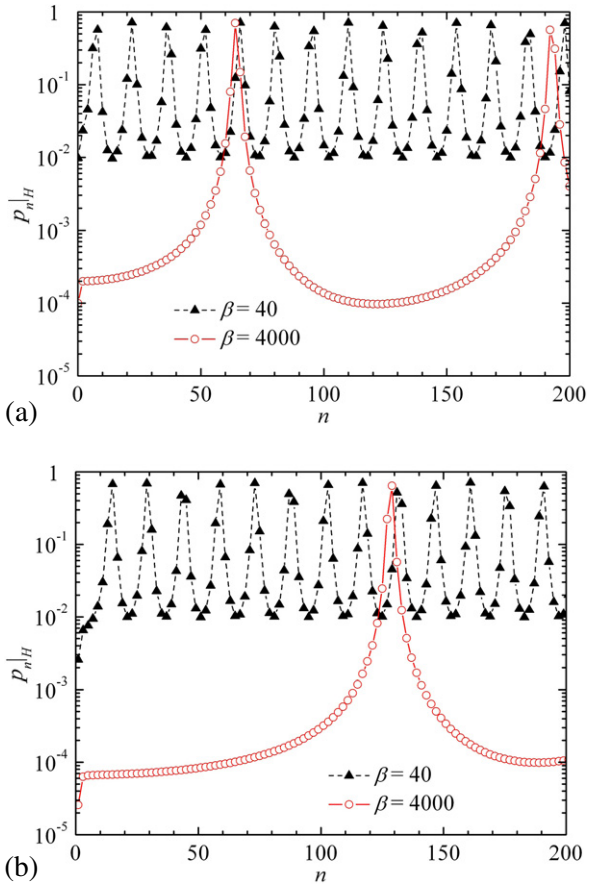

Figure 3. The probability $p_{n,\mu}|_{\mathrm{H}}$ in the H region versus quantum number n, with $K_\mu = 0$, shown in (a) for the even-parity states and in (b) for the odd-parity states. Parameters except β are $L = H/2$, $\alpha = 10$, $\gamma = 2$. Two values of β are used—$\beta = 40$ (black triangles) and $\beta = 4000$ (empty circles).

Since $C(\vec{r}, \vec{r})$ is weighed by $|\Psi_\beta(r)|^2$ as shown in equation (3.2), equations (3.6*a*)–(3.6*d*) suggest, for the backscattering $C(\vec{r}_{\mathrm{H}}, \vec{r}_{\mathrm{H}})$ with $\vec{r}_{\mathrm{H}} \in$ H region, that H states are dominant while L states make hardly any contribution. The degree of dominance increases with increasing α/γ, β and χ. One can go through the same argument and show that, for the backscattering $C(\vec{r}_{\mathrm{L}}, \vec{r}_{\mathrm{L}})$ with $\vec{r}_{\mathrm{L}} \in$ L region, L states make a dominant contribution.

It is possible to evaluate $C(\vec{r}, \vec{r})$ in equation (3.2) with $\lambda_{n,\mu}$s and $\psi_{n,\mu}$s obtained by directly solving equations (3.5*a*) and (3.5*b*). However, we employ an approximation method as follows. In summary, we solve $\lambda_{n,\mu}$s and $\psi_{n,\mu}$s numerically from equations (3.5*a*) and (3.5*b*) at $K_\mu = 0$ only. For $K_\mu \neq 0$, $D(x)K_\mu^2$ appears in equation (3.4) as a 'potential barrier' and is treated perturbatively. It leads to approximate expressions for $\lambda_{n,\mu}$ and $p_{n,\mu}|_{\mathrm{H}}$ which facilitate the evaluation of $C(\vec{r}, \vec{r})$. Because of the presence of a potential barrier, two distinct cases, namely, above-barrier and below-barrier states, are separately considered below.

In the above-barrier case, where

$$\lambda_{n,\mu} > D_{\mathrm{H}} K_\mu^2,$$

equation (3.4) gives a sinusoidal wave solution in the H region. We take approximately

$$p_{n,\mu}|_{\mathrm{H/L}} \approx p_{n,K_\mu=0}|_{\mathrm{H/L}} \text{ (above barrier)} \tag{3.7a}$$

$$\lambda_{n,\mu} \approx \lambda_{n,K_\mu=0} + D_{\mathrm{eff}}(n)K_\mu^2 \text{ (above barrier)}. \tag{3.7b}$$

Equation (3.7*b*) has the interpretation of separating entangled degrees of freedom into independent ones and approximating the total 'energy' as a sum of the individual ones (e.g. $\lambda_{n,K_\mu=0}$ for the x motion and $D_{\mathrm{eff}}(n)K_\mu^2$ for the yz motion). The effective diffusivity for the yz motion is

$$D_{\mathrm{eff}}(n) \equiv p_{n,K_\mu=0}|_{\mathrm{L}} D_{\mathrm{L}} + p_{n,K_\mu=0}|_{\mathrm{H}} D_{\mathrm{H}} \tag{3.7c}$$

which is an average of diffusivities weighted by the corresponding probabilities. Note that, with equation (3.7*b*), the above-barrier condition, $\lambda_{n,\mu} > D_{\mathrm{H}}K_\mu^2$, can be re-expressed as

$$\lambda_{n,K_{\mu=0}} > [D_{\mathrm{H}} - D_{\mathrm{eff}}(n)]K_\mu^2.$$

On the other hand, in the below-barrier case, we have

$$D_{\mathrm{L}}K_\mu^2 < \lambda_{n,\mu} < D_{\mathrm{H}}K_\mu^2,$$

and the wavefunction decays exponentially in the H region. $p_{n,\mu}|_{\mathrm{H}} \ll 1$ for the below-barrier states, and thus they are all L states. We take approximately

$$\lambda_{n,\mu} \approx \lambda_{n,K_\mu=0} + D_{\mathrm{eff}}(n)K_\mu^2 \quad \text{(below barrier L-states)} \tag{3.7d}$$

$$\begin{aligned} p_{n,\mu}|_{\mathrm{H}} &\approx p_{n,K_\mu=0}|_{\mathrm{H}} f_{n,\mu} \\ p_{n,\mu}|_{\mathrm{L}} &= 1 - p_{n,\mu}|_{\mathrm{H}} \end{aligned} \quad \text{(below barrier L-states)} \tag{3.7e}$$

where

$$f_{n,\mu} \equiv \frac{\sinh(\gamma_{n,\mu}^{(\mathrm{H})}H)/(\gamma_{n,\mu}^{(\mathrm{H})}H) \pm 1}{\cosh(\gamma_{n,\mu}^{(\mathrm{H})}H) \pm 1} \leqslant 1$$

appears as an extra factor in comparison with equation (3.7*a*), with '+' used for even-parity and '−' for odd-parity states, and $\gamma_{n,\mu}^{(\mathrm{H})}$ is determined by the equation $\lambda_{n,\mu} = D_{\mathrm{H}}[-(\gamma_{n,\mu}^{(\mathrm{H})})^2 + K_\mu^2]$. With (3.7*d*), the below-barrier condition is re-expressed as

$$\lambda_{n,K_\mu=0} < (D_{\mathrm{H}} - D_{\mathrm{eff}}(n))K_\mu^2.$$

4. Qualitative picture and formulae for the calculation of δG and MC

Section 4 consists of two sections. We firstly give a qualitative picture of δG and MC in section 4.1 and show how saturation of δG/MC may arise for a sandwich structure. The picture presented can be verified with the analytical result derived in section 5. We then present quantitative expressions within perturbation theory in section 4.2 for the calculation of δG/MC. Numerical results presented in section 6 are obtained with the formulae in section 4.2.

4.1. Qualitative picture of δG/MC and condition for saturation

We first discuss the classical conductance of the structure. Given the strong contrast $G_{\mathrm{L}}/G_{\mathrm{H}} \ll 1$, the current is mainly confined in the H layer, with a small amount of leakage current in the L region. The ratio of the currents in H and L regions is estimated to be $I_{\mathrm{L}}/I_{\mathrm{H}} \sim O(G_{\mathrm{L}}/G_{\mathrm{H}})$, previously noted in the discussion of figure 2. Equivalently, the total conductance is $G \approx G_{\mathrm{H}} + O(G_{\mathrm{L}})$. Following it, the conductance correction is thus

$$\delta G \approx \delta G_{\mathrm{H}} + O(\delta G_{\mathrm{L}}) \approx H\langle\delta\sigma(\vec{r}_{\mathrm{H}})\rangle + O\left[L\langle\delta\sigma(\vec{r}_{\mathrm{L}})\rangle\right]$$

where $\langle\delta\sigma(\vec{r}_{\mathrm{H}})\rangle$ means the average of $\delta\sigma(\vec{r}_{\mathrm{H}})$ over the H layer, for example. Similarly, the MC, defined as $\Delta G(B) \equiv \delta G|_{B\neq 0} - \delta G|_{B=0}$, is approximately

$$\Delta G(B) \approx \Delta G_{\mathrm{H}}(B) + O(\Delta G_{\mathrm{L}}(B))$$

where $\Delta G_{\mathrm{H}}(B) \equiv \delta G_{\mathrm{H}}|_{B\neq 0} - \delta G_{\mathrm{H}}|_{B=0}$ and $\Delta G_{\mathrm{L}}(B) \equiv \delta G_{\mathrm{L}}|_{B\neq 0} - \delta G_{\mathrm{L}}|_{B=0}$.

To simplify the analysis of δG and MC as functions of temperature, we divide the temperature into three regimes with the characteristic temperatures, T_{H} and T_{L}, which are determined as follows:

$$1/\tau_\varphi^{(\mathrm{H})}(T) \sim D_{\mathrm{H}}/H^2 \qquad \text{at } T = T_{\mathrm{H}},$$

$$1/\tau_\varphi^{(\mathrm{L})}(T) \sim 1/\tau_{\mathrm{L}} \qquad \text{at } T = T_{\mathrm{L}},$$

where $\tau_{\mathrm{L}} \equiv l_{\mathrm{L}}/v_{\mathrm{L}}$ is the elastic mean free time of electrons in the L region. As shall become obvious below, a sufficient condition for the occurrence of saturation is

$$T_{\mathrm{L}} < T_{\mathrm{H}}. \tag{SAT}$$

In the case where $1/\tau_\varphi^{(\mathrm{H})}(T) \propto 1/\tau_\varphi^{(\mathrm{L})}(T) \propto T^p (p > 0)$, the condition (SAT) can easily be shown to translate into $\frac{(1/\tau_{\mathrm{L}})}{(D_{\mathrm{H}}/H^2)} < \frac{\tau_\varphi^{(\mathrm{H})}}{\tau_\varphi^{(\mathrm{L})}}$, or

$$\gamma^2/\beta\chi^2 < \frac{\tau_\varphi^{(\mathrm{H})}}{\tau_\varphi^{(\mathrm{L})}}. \tag{SAT$'$}$$

In the following discussion, we assume (SAT) is met and proceed to discuss δG and MC in the three regimes, namely $T_{\mathrm{H}} < T$, $T_{\mathrm{L}} < T \leqslant T_{\mathrm{H}}$ and $T \leqslant T_{\mathrm{L}}$

We first consider δG for the first two regimes where $T_{\mathrm{L}} < T$, or $1/\tau_{\mathrm{L}} < 1/\tau_\varphi^{(\mathrm{L})}$ in terms of $1/\tau_\varphi^{(\mathrm{L})}(T)$. At such $1/\tau_\varphi^{(\mathrm{L})}$, there is not enough time for (elastic) backscattering in the L region to occur yet, and hence $\delta G_{\mathrm{L}} \sim 0$. So we have

$$\delta G \approx H\,\langle\delta\sigma(\vec{r}_{\mathrm{H}})\rangle \propto \sum_\beta \frac{\left\langle|\Psi_\beta(\vec{r}_{\mathrm{H}})|^2 v(x_{\mathrm{H}})/\tau(x_{\mathrm{H}})\right\rangle}{\lambda_\beta + 1/\tau_\varphi^{(\beta)}}$$

$$= \langle C(\vec{r}_{\mathrm{H}}, \vec{r}_{\mathrm{H}})\rangle.$$

Now, we analyze $C(\vec{r}_{\mathrm{H}}, \vec{r}_{\mathrm{H}})$. It contains contributions from all eigenstates and we pay attention firstly to that of the zero mode $\lambda_\beta = 0$. One can easily verify the existence of

zero mode by substituting the expressions $\lambda_{n=0,K_\mu=0} = 0$ and $\psi_{n=0,K_\mu=0}(x) \propto 1/\nu(x)$ into equation (3.4). Generally speaking, the zero mode always exists for a diffusion-type equation and it results in the function $C(\vec{r},\vec{r})$, which has been called the diffusion pole in the literature. In the case of a homogeneous system, the solution causes $C(\vec{r},\vec{r})$ to diverge at zero temperature (where $1/\tau_\varphi = 0$). However, in our case of a sandwich structure, the zero mode with $\psi_{n=0,K_\mu=0}(x)[\propto 1/\nu(x)]$ has the probability distribution primarily located in the L region, and one can easily derive that

$$p_{n=0,K_\mu=0}|_{\mathrm{L}} = 1/(1+\gamma/2\alpha\beta\chi^2)$$

$$p_{n=0,K_\mu=0}|_{\mathrm{H}} = (\gamma/2\alpha\beta\chi^2)/(1+\gamma/2\alpha\beta\chi^2).$$

Given the parameters either $\beta \gg 1$, $\alpha,\gamma > 1$, $\alpha/\gamma > 1$, $\chi \geqslant O(1)$ or $\beta \geqslant O(1)$, $\alpha,\gamma > 1$, $\alpha/\gamma > 1$, $\chi \gg 1$ as specified earlier, the above expressions show $p_{n=0,K_\mu=0}|_{\mathrm{L}} \approx 1$ and $p_{n=0,K_\mu=0}|_{\mathrm{H}} \ll 1$, which implies that the zero mode is an L state. As noted earlier, such a state hardly contributes to $C(\vec{r}_{\mathrm{H}},\vec{r}_{\mathrm{H}})$ and, consequently, the associated divergence is suppressed for the sandwich structure in the regime $T_{\mathrm{L}} < T$.

With the pole (and all other L-state) contribution thus being negligible, $C(\vec{r}_{\mathrm{H}},\vec{r}_{\mathrm{H}})$ is primarily determined by the spectrum of H states, which starts at the finite value $\lambda^{(\mathrm{H})}_{\mathrm{min}} = O(D_{\mathrm{H}}/H^2)$ corresponding to the lowest standing wave in the H layer. Therefore, for $T_{\mathrm{L}} < T$, we write approximately

$$\delta G \propto \langle C(\vec{r}_{\mathrm{H}},\vec{r}_{\mathrm{H}})\rangle \propto \sum_{\substack{\lambda_\beta \geqslant \lambda^{(\mathrm{H})}_{\mathrm{min}} \\ \beta=\text{H-states}}} \frac{\left\langle |\Psi_\beta(\vec{r}_{\mathrm{H}})|^2 v(x_{\mathrm{H}})/\tau(x_{\mathrm{H}})\right\rangle}{\lambda_\beta + 1/\tau^{(\mathrm{H})}_\varphi}.$$

We further rewrite it as

$$\delta G \propto \sum_{\substack{\lambda'_\beta \geqslant 0 \\ \beta=\text{H-states}}} \frac{\left\langle |\Psi_\beta(\vec{r}_{\mathrm{H}})|^2 v(x_{\mathrm{H}})/\tau(x_{\mathrm{H}})\right\rangle}{\lambda''_\beta + 1/\tau^{(\mathrm{eff})}_\varphi + 1/\tau^{(\mathrm{H})}_\varphi} \qquad (T_{\mathrm{L}} < T) \tag{4.1.1}$$

where $\lambda''_\beta = \lambda_\beta - 1/\tau^{(\mathrm{eff})}_\varphi$ and

$$1/\tau^{(\mathrm{eff})}_\varphi \equiv \lambda^{(\mathrm{H})}_{\mathrm{min}} \sim D_{\mathrm{H}}/H^2. \tag{4.1.2}$$

The regime of $T_H < T$. We now apply equation (4.1.1) firstly to the regime $T_{\mathrm{H}} < T$, or $D_{\mathrm{H}}/H^2 (\sim 1/\tau^{(\mathrm{eff})}_\varphi) < 1/\tau^{(\mathrm{H})}_\varphi$ in terms of $1/\tau^{(\mathrm{H})}_\varphi(T)$. With $1/\tau^{(\mathrm{H})}_\varphi > 1/\tau^{(\mathrm{eff})}_\varphi$, one can drop $1/\tau^{(\mathrm{eff})}_\varphi$ in the rhs of equation (4.1.1) without qualitatively modifying the physics it represents, and so

$$\delta G \propto \sum_{\substack{\lambda''_\beta \geqslant 0 \\ \beta=\text{H-states}}} \frac{\left\langle |\Psi_\beta(\vec{r}_{\mathrm{H}})|^2 v(x_{\mathrm{H}})/\tau(x_{\mathrm{H}})\right\rangle}{\lambda''_\beta + 1/\tau^{(\mathrm{H})}_\varphi} \qquad (T_{\mathrm{H}} < T). \tag{4.1.3}$$

Now, it is important to note that the above sum in (4.1.3) simulates basically the Cooperon of an isolated H film (with thickness $= H$) at high temperatures. This can be understood as follows. For the film, the corresponding eigenvalues are exactly $D_{\mathrm{H}} n^2\pi^2/H^2$, $n = 0, 1, 2, \ldots$, which are approximately λ''_βs of H states in (4.1.3). Similarly, the eigenfunctions of the film are exactly standing waves (plus the zero mode whose wavefunction is $\Psi(\vec{r}) =$ constant), which may, too, be approximated by Ψ_βs in (4.1.3). Therefore, the sum in (4.1.3) represents nearly the Cooperon of the film. With this result, one can apply the film theory of weak localization (e.g. [2]) to the sandwich structure. For $T_{\mathrm{H}} < T$, we thus conclude that δG is moderately and MC is strongly T-dependent.

The regime of $T_L < T \leqslant T_H$. Next, we apply equation (4.1.1) to the regime $T_{\mathrm{L}} < T \leqslant T_{\mathrm{H}}$, or $1/\tau_{\mathrm{L}} < 1/\tau^{(\mathrm{L})}_\varphi$ together with $1/\tau^{(\mathrm{H})}_\varphi \leqslant D_{\mathrm{H}}/H^2 (\sim 1/\tau^{(\mathrm{eff})}_\varphi)$, in terms of $1/\tau^{(\mathrm{L})}_\varphi(T)$ and $1/\tau^{(\mathrm{H})}_\varphi(T)$. Since $1/\tau^{(\mathrm{H})}_\varphi \leqslant 1/\tau^{(\mathrm{eff})}_\varphi$, one can drop $1/\tau^{(\mathrm{H})}_\varphi$ in the rhs of equation (4.1.1) without modifying the physics, which gives

$$\delta G \propto \sum_{\substack{\lambda''_\beta \geqslant 0 \\ \beta=\text{H-states}}} \frac{\left\langle |\Psi_\beta(\vec{r}_{\mathrm{H}})|^2 v(x_{\mathrm{H}})/\tau(x_{\mathrm{H}})\right\rangle}{\lambda''_\beta + 1/\tau^{(\mathrm{eff})}_\varphi} \qquad (T_{\mathrm{L}} < T \leqslant T_{\mathrm{H}}). \tag{4.1.4}$$

Now, the rhs of the last expression simulates the Cooperon of an isolated H film with a constant phase breaking rate $1/\tau^{(\mathrm{eff})}_\varphi \sim D_{\mathrm{H}}/H^2$. It implies that both δG and MC show weak T dependence (i.e. saturation).

The foregoing discussion for the two regimes, $T_{\mathrm{H}} < T$ and $T_{\mathrm{L}} < T \leqslant T_{\mathrm{H}}$, also implies that T_{H} at which $1/\tau^{(\mathrm{H})}_\varphi \sim O(D_{\mathrm{H}}/H^2)$ is a characteristic temperature for the onset of MC saturation when the temperature gradually decreases.

The regime of $T \leqslant T_L$. Now we discuss what happens when we enter the regime of extremely low temperatures where $T \leqslant T_{\mathrm{L}}$ or $1/\tau^{(\mathrm{L})}_\varphi \leqslant 1/\tau_{\mathrm{L}}$. In this case, backscattering in the L region generally begins to occur and increases with decreasing temperature. δG_{L} is not negligible, and thus $\delta G \approx \delta G_{\mathrm{H}} + O(\delta G_{\mathrm{L}})$ and $\Delta G \approx \Delta G_{\mathrm{H}} + O(\Delta G_{\mathrm{L}})$, with both contributions necessarily included. Since $T \leqslant T_{\mathrm{H}}$, equation (4.1.4) still applies for δG_{H}. Thus, one has $\delta G_{\mathrm{H}} = \delta G_{\mathrm{H}}$ (saturated) and, similarly, $\Delta G_{\mathrm{H}} = \Delta G_{\mathrm{H}}$ (saturated), both showing weak T dependence. On the other hand, δG_{L} and ΔG_{L} may or may not be T-sensitive. It depends on the structure and is discussed below. For reference, we write approximately δG_{L} here:

$$\delta G_{\mathrm{L}} \propto \sum_{\substack{\lambda_\beta \geqslant 0 \\ \beta\in\text{L-states}}} \frac{\left\langle |\Psi_\beta(\vec{r}_{\mathrm{L}})|^2 v(x_{\mathrm{L}})/\tau(x_{\mathrm{L}})\right\rangle}{\lambda_\beta + 1/\tau^{(\mathrm{L})}_\varphi} \qquad (T \leqslant T_{\mathrm{L}}) \tag{4.1.5}$$

where only the dominant contribution (from L states) is kept.

Film-like structures. In a film-like structure, δG_{L} in (4.1.5) is basically the quantum correction of an isolated L film at extremely low temperatures, which is T-sensitive, and thus $\delta G[\approx \delta G_{\mathrm{H}}(\text{saturated}) + O(\delta G_{\mathrm{L}})]$ increases sharply for $T \leqslant T_{\mathrm{L}}$. So does $\Delta G[\approx \Delta G_{\mathrm{H}}(\text{saturated}) + O(\Delta G_{\mathrm{L}})]$.

Bulk-like structures. On the other hand, if the structure is bulk-like, δG_{L} in (4.1.5) is basically the quantum correction of a 3D L bulk at extremely low temperatures. δG_{L} is insensitive to T variation, and so is the total correction δG. Saturation of

δG thus persists even for $T \leqslant T_{\rm L}$ down to 0 K. As for $\Delta G_{\rm L}$, it is generally strongly T-dependent, as is typical of a 3D system, and thus the total ΔG is likely to increase sharply for $T \leqslant T_{\rm L}$. However, in the limit of a clean L bulk where $l_{\rm L} \sim L \sim L_{yz}$, backscattering interference in the L region hardly occurs. $\Delta G_{\rm L}$ is nearly zero and thus the total MC saturates at $\Delta G \sim \Delta G_{\rm H}$ (saturated) for $T \leqslant T_{\rm L}$ down to 0 K.

4.2. Formulas for the calculation of δG and MC

We include both $\delta G_{\rm H}$ and $\delta G_{\rm L}$ in the analysis and derive quantitative expressions for δG and MC within perturbation theory. We simply take $\delta G[\approx \delta G_{\rm H} + O(\delta G_{\rm L})]$ to be $\delta G_{\rm H} + \delta G_{\rm L}$, within logarithmic accuracy. We have the following conductance correction due to backscattering interference:

$$\begin{aligned}\delta G_i &= t_i \langle \delta\sigma(\vec{r}_i)\rangle \\ &= -G_0 \frac{D_i}{L_{yz}^2} \sum_{n,\mu} \frac{\int \mathrm{d}x_i\,\mathrm{d}y\,\mathrm{d}z |\Psi_{n,\mu}(x_i, y, z)|^2 v(x_i)}{\lambda_{n,\mu} + 1/\tau_\varphi^{(n,\mu)}} \\ &= \begin{cases} -G_0 D_i \displaystyle\sum_n \int \frac{\mathrm{d}^2 K_\mu}{(2\pi)^2} \frac{p_{n,K_\mu}|_i}{\lambda_{n,k_y,k_z} + 1/\tau_\varphi^{(n,\mu)}} \\ \qquad \text{for } B = 0 \\ -G_0 D_i g_B \displaystyle\sum_{n,\mu} \frac{p_{n,\mu}|_i}{\lambda_{n,\mu}(B) + 1/\tau_\varphi^{(n,\mu)}} \\ \qquad \text{for } B \neq 0 \end{cases} \end{aligned} \tag{4.2.1}$$

where the subscript i = L, H, t_i = thickness of the i region, $g_B = 2eB/hc$ is the degeneracy per unit area for each Landau level, and $p_{n,K_\mu}|_i$ and $p_{n,\mu}|_i$ are the integrated probability $\int \mathrm{d}x_i\,\mathrm{d}y\,\mathrm{d}z|\Psi_{n,\mu}(x_i, y, z)|^2 v(x_i)$ in the i region. (The symbols μ and K_μ are used interchangeably throughout this presentation.) The above equation shows explicitly the dependence of δG_i on $p_{n,\mu}|_i$, thus favoring those states with large probability in the i layer, namely the i states. We further decompose

$$\begin{aligned}\delta G_i = {} & \delta G_i^{(\rm H)}(\text{above barrier}) + \delta G_i^{(\rm L)}(\text{above barrier}) \\ & + \delta G_i^{(\rm L)}(\text{below barrier})\end{aligned}$$

where $\delta G_i^{(\rm H)}$ (above barrier) for example, means the contribution from above-barrier H states. Next, we treat each part separately.

With the approximation (3.7*a*)–(3.7*c*), equation (4.2.1) can be simplified, e.g. the integral $\int \mathrm{d}^2 K_\mu$ in equation (4.2.1) (with $B = 0$) can be analytically evaluated for $\delta G_i^{(\rm H/L)}$(above barrier), resulting in

$$\begin{aligned}\delta G_i^{(j)}(\text{above barrier}) &\approx -G_0 D_i \\ &\quad \times \sum_{(n,\mu)\in j\text{-states}} \int \frac{\mathrm{d}^2 K_\mu}{(2\pi)^2} \frac{p_{n,K_\mu=0}|_i}{\lambda_{n,K_\mu=0} + D_{\rm eff}(n) K_\mu^2 + 1/\tau_\phi^{(j)}} \\ &= -G_0 \sum_{n\in j\text{-state}s}^{N_{\max}^{(j)}} \frac{p_{n,K_\mu=0}|_i}{4\pi} \frac{D_i}{D_{\rm eff}(n)} \ln\left(\left(l_\varphi^*(n)\right)^2/l_n^2 + 1\right)\end{aligned} \tag{4.2.2}$$

where $i = \rm H, L$, $j = \rm H, L$, and $(l_\varphi^*(n))^2 \equiv D_{\rm eff}(n)/(\lambda_{n,K_\mu=0} + 1/\tau_\phi^{(j)})$. π/l_n is the upper bound of the integral $\int \mathrm{d}^2 K_\mu$ to be discussed below. For $B \neq 0$, we introduce the magnetic length l_B defined by $l_B^2 \equiv (2\pi g_B)^{-1} = \hbar c/2eB$ and write

$$\begin{aligned}&\delta G_i^{(j)}(\text{above barrier}) \\ &\quad \approx -G_0 D_i g_B \sum_{(n,\mu)\in j\text{-states}} \frac{p_{n,K_\mu=0}|_i}{\lambda_{n,K_\mu=0} + D_{\rm eff}(n) K_\mu^2 + 1/\tau_\phi^{(j)}} \\ &\quad = -G_0 g_B \sum_{n\in j\text{-states}}^{N_{\max}^{(j)}} \frac{p_{n,K_\mu=0}|_i}{2\pi} \frac{D_i}{D_{\rm eff}(n)} \\ &\qquad \times \sum_{\mu}^{\mu_{\max}^{(j)}} \frac{1}{(2\mu+1) + (l_B/l_\varphi^*(n))^2}.\end{aligned} \tag{4.2.3}$$

The indices (n, μ) of the states to be included in $\delta G_i^{(\rm H/L)}$ (above barrier) are determined by the following conditions, namely that (i) *wavelength of the state > mean free path* and that (ii) the state is above the barrier. Accordingly, the upper bound $N_{\max}^{(j)}$ for the sum $\sum_n$ in equations (4.2.2) and (4.2.3) satisfies

$$\lambda_{N_{\max}^{(j)}, K_\mu=0} = D_j \pi^2/l_j^2,$$

where $j = H$ (for H states) and L (for L states). For a given n, the integral $\int \mathrm{d}^2 K_\mu$ in equation (4.2.2) (or the sum $\sum_\mu$ in equation (4.2.3)) is restricted to the interval

$$\left\{0, K_{\mu_{\max}^{(j)}}\right\}.$$

The upper bound, $K_{\mu_{\max}^{(j)}}$, is n-dependent and determined by

$$\pi/l_n \equiv K_{\mu_{\max}^{(j)}} = \min\left[\pi/l_j, [\lambda_{n,K_\mu=0}/(D_{\rm H} - D_{\rm eff}(n))]^{1/2}\right],$$

where $j = H$ (for H states) and L (for L states).

As for the below-barrier contribution, $\delta G_i^{(\rm L)}$ (below barrier), one resorts to equation (4.2.1), with the approximate expressions (3.7*d*) and (3.7*e*) for $\lambda_{n,\mu}$ and $p_{n,\mu}|_i$. The upper bound $N_{\max}^{(j)}$ remains the same as that given above. However, the integral $\int \mathrm{d}^2 K_\mu$ (or the sum $\sum_\mu$) is restricted to the interval

$$\left\{K_{\mu_{\max}^{(j)}}, \pi/l_j\right\}.$$

We now discuss the calculation of MC. Magnetoconductance, defined as $\Delta G(B) \equiv \delta G|_{B\neq 0} - \delta G|_{B=0}$, can be evaluated directly with the values of $\delta G|_{B\neq 0}$ and $\delta G|_{B=0}$. However, simplification is possible in the case of weak magnetic fields, as follows. Firstly, it is convenient to write

$$\begin{aligned}\Delta G_i^{(j)}(B) &\equiv \delta G_i^{(j)}|_{B\neq 0} - \delta G_i^{(j)}|_{B=0} \\ &= G_0 D_i \sum_{n\in j\text{-states}}^{N_{\max}^{(j)}} \sum_{\mu}^{\mu_{\max}^{(j)}} \Delta_{n,\mu}\end{aligned}$$

where

$$\begin{aligned}\Delta_{n,\mu} \equiv \int_{Q_\mu}^{Q_{\mu+1}} \frac{\mathrm{d}^2 \vec{k}_\parallel}{(2\pi)^2} \Bigg\{ & \frac{p_{n,\mu}|_i}{\lambda_{n,K_\mu=0} + D_{\rm eff}(n) K_\mu^2 + 1/\tau_\phi^{(j)}} \\ & - \frac{p_{n,\vec{k}_\parallel=0}|_i}{\lambda_{n,K_\mu=0} + D_{\rm eff}(n) k_\parallel^2 + 1/\tau_\varphi^{(j)}} \Bigg\}\end{aligned}$$

with $Q_\mu^2 \equiv 4eB\mu/\hbar c$ and $K_\mu^2 \equiv 4eB(\mu+1/2)/\hbar c$. For the above-barrier contribution, $p_{n,\mu}|_i = p_{n,\vec{k}_\parallel=0}|_i$ according to equation (3.7*a*). The probability factor can thus be moved out of the integral $\Delta_{n,\mu}$ and evaluation of the integral gives (correct to $O(B^2)$)

$$\sum_{\mu}^{\mu_{\max}^{(j)}} \Delta_{n,\mu} \approx \frac{p_{n,K_\mu=0}|_i}{24\pi D_{\rm eff}(n)} \left(\left(l_\phi^*(n)\right)^2 / l_B^2 \right)^2$$

above the barrier.

Thus

$$\Delta G_i^{(j)}(B) \approx G_0 \sum_{n\in j\text{-states}}^{N_{\max}^{(j)}} \frac{p_{n,K_\mu=0}|_i}{24\pi} \frac{D_i}{D_{\rm eff}(n)} \left(\left(l_\phi^*(n)\right)^2 / l_B^2 \right)^2$$

above the barrier (4.2.4)

in the case of weak magnetic fields.

In summary, we calculate δG with equations (4.2.1) (for the below-barrier contribution) and (4.2.2) and (4.2.3) (for the above-barrier contribution). On the other hand, MC is calculated with equations (4.2.1) (for the below-barrier contribution) and (4.2.4) (for the above-barrier contribution). Numerical results presented in section 6 are obtained in this way.

Since our calculation will be compared with that of an isolated H film in section 6, we briefly remark on the calculation of δG and MC for a film. The isolated film is obviously a special case of a sandwich structure and, as such, can be treated with the theory here. In the film case, the corresponding eigenstates are H states and the zero mode, and thus the film formulae can be obtained by setting in equations (4.2.2), (4.2.3) and (4.2.4)

$$D_{\rm eff}(n) = D_{\rm H}, \qquad p_{n,K_\mu=0}|_{\rm H} = 1,$$

$$\lambda_{n,K_\mu=0} = D_{\rm H}(n\pi/H)^2, \qquad n = 0, 1, 2, \ldots$$

and the upper bounds

$$\lambda_{N_{\max}^{(\rm H)},K_\mu=0} = D_{\rm H}\pi^2/l_{\rm H}^2$$

$$K_{\mu_{\max}^{(\rm H)}} = \pi/l_{\rm H}.$$

5. Analytical results of δG and MC

Previously we have chosen the parameters either $\beta \gg 1$, $\alpha, \gamma > 1$, $\alpha/\gamma > 1$, $\chi \geqslant O(1)$ (for film-like structures), or $\beta \geqslant O(1)$, $\alpha, \gamma > 1$, $\alpha/\gamma > 1$, $\chi \gg 1$ (for bulk-like structures). In this section, we shall tighten the parametric range a little and make it either $\beta \gg 1$, $\alpha, \gamma > 1$, $\alpha/\gamma > 1$, $\chi > 1$, or $\beta > 1$, $\alpha, \gamma > 1$, $\alpha/\gamma > 1$, $\chi \gg 1$. With this modification, it is possible to proceed further with the formulae presented in section 4.2 and make analytical estimates of δG and MC within logarithmic accuracy. We focus on δG in section 5.1 and MC in section 5.2. The result derived below confirms the qualitative picture presented earlier in section 4.1.

5.1. Analytical estimate of δG (at $B = 0$)

We firstly compare the magnitude of various $\delta G_i^{(j)}$s. We start with the H-state contribution. According to section 4.2, we have

$$\delta G_{\rm L}^{(\rm H)} \approx -G_0 D_{\rm L} \times \sum_{(n,\mu)\in \text{H-states}} \int \frac{{\rm d}^2 K_\mu}{(2\pi)^2} \frac{p_{n,K_\mu=0}|_{\rm L}}{\lambda_{n,K_\mu=0} + D_{\rm eff}(n)K_\mu^2 + \tau_\varphi^{(H)-1}}$$

$$\delta G_{\rm H}^{(\rm H)} \approx -G_0 D_{\rm H} \times \sum_{(n,\mu)\in \text{H-states}} \int \frac{{\rm d}^2 K_\mu}{(2\pi)^2} \frac{p_{n,K_\mu=0}|_{\rm H}}{\lambda_{n,K_\mu=0} + D_{\rm eff}(n)K_\mu^2 + \tau_\varphi^{(H)-1}}.$$

It gives

$$\frac{\delta G_{\rm L}^{(\rm H)}}{\delta G_{\rm H}^{(\rm H)}} \sim \frac{D_{\rm L}}{D_{\rm H}} \left\langle \frac{p_{n,K_\mu=0}|_{\rm L}}{p_{n,K_\mu=0}|_{\rm H}} \right\rangle$$

where $\langle \frac{p_{n,K_\mu=0}|_{\rm L}}{p_{n,K_\mu=0}|_{\rm H}} \rangle$ is the typical probability ratio for H states. According to section 3, it is less than $O(\gamma/\alpha)$. Therefore

$$\frac{\delta G_{\rm L}^{(\rm H)}}{\delta G_{\rm H}^{(\rm H)}} \sim \frac{D_{\rm L}}{D_{\rm H}} \left\langle \frac{p_{n,K_\mu=0}|_{\rm L}}{p_{n\,K_\mu=0}|_{\rm H}} \right\rangle \leqslant \frac{1}{\beta}\frac{\gamma}{\alpha} < 1. \qquad (5.1.1)$$

Similarly, for the L-state contribution, we have

$$\delta G_{\rm L}^{(\rm L)} \approx -G_0 D_{\rm L} \times \sum_{(n,\mu)\in \text{L-states}} \int \frac{{\rm d}^2 K_\mu}{(2\pi)^2} \frac{p_{n,K_\mu}|_{\rm L}}{\lambda_{n,K_\mu=0} + D_{\rm eff}(n)K_\mu^2 + \tau_\varphi^{(L)-1}}$$

$$\delta G_{\rm H}^{(\rm L)} \approx -G_0 D_{\rm H} \times \sum_{(n,\mu)\in \text{L-states}} \int \frac{{\rm d}^2 K_\mu}{(2\pi)^2} \frac{p_{n,K_\mu}|_{\rm H}}{\lambda_{n,K_\mu=0} + D_{\rm eff}(n)K_\mu^2 + \tau_\varphi^{(L)-1}}.$$

It gives

$$\frac{\delta G_{\rm H}^{(\rm L)}}{\delta G_{\rm L}^{(\rm L)}} \sim \frac{D_{\rm H}}{D_{\rm L}} \left\langle \frac{p_{n,K_\mu}|_{\rm H}}{p_{n,K_\mu}|_{\rm L}} \right\rangle \leqslant \frac{\gamma}{\alpha\chi^2} < 1. \qquad (5.1.2)$$

According to equations (5.1.1) and (5.1.2), we can drop $\delta G_{\rm H}^{(\rm L)}$ and $\delta G_{\rm L}^{(\rm H)}$, and write $\delta G \sim \delta G_{\rm H}^{(\rm H)} + \delta G_{\rm L}^{(\rm L)}$ within logarithmic accuracy. We evaluate $\delta G_{\rm H}^{(\rm H)}$ first and then $\delta G_{\rm L}^{(\rm L)}$.

Calculation of $\delta G_H^{(H)}$. According to section 4, H states are all above barrier and their contribution gives

$$\delta G_{\rm H}^{(\rm H)}(\text{above barrier}) \sim -\frac{G_0}{4\pi} \times \sum_{n\in \text{H-states}} \ln \frac{\lambda_{n,K_\mu=0} + D_{\rm H}K_{\mu_{\max}^{(\rm H)}}^2 + \tau_\varphi^{(H)-1}}{\lambda_{n,K_\mu=0} + \tau_\varphi^{(H)-1}}$$

where we have taken $p_{n,K_\mu=0}|_{\rm H} \sim 1$ and $D_{\rm eff}(n) \sim D_{\rm H}$ for the H states. Moreover, we take $\lambda_{n,K_\mu=0} \sim D_{\rm H}\frac{n^2\pi^2}{H^2}$, $n = 1, 2, \ldots$ and

$$K_{\mu_{\max}^{(\rm H)}}^2 \sim \min\left[\frac{\alpha}{\gamma}\frac{n^2\pi^2}{H^2}, \frac{\pi^2}{l_{\rm H}^2}\right] = \begin{cases} \frac{\alpha}{\gamma}\frac{n^2\pi^2}{H^2} & (n < n_1) \\ \frac{\pi^2}{l_{\rm H}^2} & (n > n_1), \end{cases}$$

$n_1 \equiv \sqrt{\gamma\alpha}$.

We can thus write

$$\delta G_{\rm H}^{(\rm H)} \sim -\frac{G_0}{4\pi}\left\{\sum_{n=1}^{n_1}\ln\frac{D_{\rm H}\frac{n^2\pi^2}{H^2}\left(1+\frac{\alpha}{\gamma}\right)}{D_{\rm H}\frac{n^2\pi^2}{H^2}+\tau_\varphi^{(H)-1}} + \sum_{n=n_1+1}^{N_{\max}^{(\rm H)}}\ln\frac{D_{\rm H}\frac{\pi^2}{l_{\rm H}^2}}{D_{\rm H}\frac{n^2\pi^2}{H^2}+\tau_\varphi^{(H)-1}}\right\}$$

where $N_{\max}^{(\rm H)} = \frac{H}{l_{\rm H}} = \alpha$. Evaluating the last expression approximately, we obtain, with

$$n_\varphi^{(\rm H)} \equiv H/\sqrt{D_{\rm H}\tau_\varphi^{(\rm H)}}, \qquad \delta G_{\rm H}^{(\rm H)} \sim -\frac{G_0}{2\pi}\left\{\alpha - n_1 - n_\varphi^{(\rm H)}\right\}, \tag{5.1.3}$$

where the coefficient of each term is actually of $O(1)$ and depends on the parameters α and γ.

For the regime $T_{\rm L} < T$, where $\delta G_{\rm L}^{(\rm L)} \sim 0$ and $\delta G \sim \delta G_{\rm H}^{(\rm H)}$, equation (5.1.3) shows weak to moderate T dependence for δG due to the term $n_\varphi^{(\rm H)}$, in agreement with the qualitative discussion in section 4.1. Moreover, it also gives the saturated value, at small $n_\varphi^{(\rm H)}$, with

$$\delta G(\text{saturated}) \sim -\frac{G_0}{2\pi}\{\alpha - n_1\}.$$

Calculation of $\delta G_L^{(L)}$. We calculate $\delta G_{\rm L}^{(\rm L)}$ in the regime $T \leqslant T_{\rm L}$. We combine $\delta G_{\rm L}^{(\rm L)}$(above barrier) and $\delta G_{\rm L}^{(\rm L)}$(below barrier) given in section 4.2 and write approximately

$$\delta G_{\rm L}^{(\rm L)} \sim \frac{G_0}{4\pi}\sum_{n=0}^{N_{\max}^{(\rm L)}}\ln\frac{D_{\rm L}\frac{n^2\pi^2}{L^2}+D_{\rm L}\frac{\pi^2}{l_{\rm H}^2}+\tau_\varphi^{(L)-1}}{D_{\rm L}\frac{n^2\pi^2}{L^2}+\tau_\varphi^{(L)-1}}$$

where $N_{\max}^{(\rm L)} = \frac{L}{l_{\rm L}} = \gamma$ and we have taken $p_{n,K_\mu=0}|_{\rm L} \sim 1$, $D_{\rm eff}(n) \sim D_{\rm L}$ and $\lambda_{n,K_\mu=0} \sim D_{\rm L}\frac{n^2\pi^2}{L^2}$, $n = 0, 1, 2, \ldots$ for L states. Evaluating the expression approximately, we obtain, with $n_\varphi^{(\rm L)} \equiv L/\sqrt{D_{\rm L}\tau_\varphi^{(\rm L)}}$

$$\delta G_{\rm L}^{(\rm L)} \sim -\frac{G_0}{2\pi}\left\{\gamma - n_\varphi^{(\rm L)} + \frac{1}{2}\ln\frac{\tau_\varphi^{(\rm L)}}{\tau_{\rm L}}\right\} \tag{5.1.4}$$

where the coefficient of each term is actually of $O(1)$. The last logarithmic term derives from the zero-mode L state and describes the conductance correction of a 2D film, while the first two terms describe the conductance correction of an L bulk. The bulk terms dominate at high $1/\tau_\varphi^{(\rm L)}$ while the film term does so at low $1/\tau_\varphi^{(\rm L)}$. The crossover from bulk-like to film-like behavior occurs at low $1/\tau_\varphi^{(\rm L)}(crossover)$ (where $n_\varphi^{(\rm L)} \sim 0$), with

$$\tau_\varphi^{(\rm L)}(\text{cross over}) \sim \tau_{\rm L}\exp(2\gamma) > \tau_{\rm L}\gamma^2 \sim L^2/D_{\rm L}. \tag{5.1.5}$$

The last result shows that $\tau_\varphi^{(\rm L)}$(crossover) is longer than the time a particle takes to diffuse across the L region (5.1.5) which determines the crossover temperature by the equation

$$\tau_\varphi^{(\rm L)}(T_{\rm crossover}) \sim \tau_\varphi^{(\rm L)}(\text{crossover}).$$

Total conductance correction δG. One can combine the results (5.1.3) and (5.1.4) to obtain $\delta G \sim \delta G_{\rm H}^{(\rm H)} + \delta G_{\rm L}^{(\rm L)}$ and verify the overall low-temperature behavior of δG discussed in section 4.1. We make only two remarks. Firstly, the additional contribution of $\delta G_{\rm L}^{(\rm L)}$ to δG for $T \leqslant T_{\rm L}$ gives an increase in δG, with the increase being described by equation (5.1.4). Secondly, we discuss the condition for zero-temperature saturation of δG. Apart from $\tau_\varphi^{(\rm L)}$(crossover) given in equation (5.1.5), we note that another important timescale is the cutoff value of phase breaking time for a finite-size system, which is $\tau_{yz}^{(\rm c)} \sim L_{yz}^2/D_{\rm L}$ (for diffusion from one electrode across the structure to the other electrode). For a bulk-like sandwich structure , $L \sim L_{yz}$ and $\tau_{yz}^{(\rm c)} \sim L^2/D_{\rm L}$. Thus, $\tau_{yz}^{(\rm c)} < \tau_\varphi^{(\rm L)}$(crossover) according to equation (5.1.5) and the crossover does not happen. In other words, the system remains bulk-like even down to 0 K with a saturated $\delta G \sim -\frac{G_0}{2\pi}(\alpha + \gamma - n_1 - n_\varphi^{(\rm L)})$ according to equations (5.1.3) and (5.1.4), where $n_\varphi^{(\rm L)}$ is evaluated at $\tau_{yz}^{(\rm c)}$. On the other hand, for a film-like structure, $L \ll L_{yz}$ and $\tau_{yz}^{(\rm c)} > \tau_\varphi^{(\rm L)}$(crossover). The system eventually crosses over at $T_{\rm crossover}$, with δG diverging as $\ln(\tau_\varphi^{(\rm L)}/\tau_{\rm L})$ for $T < T_{\rm crossover}$ according to equation (5.1.4).

5.2. Analytical estimate of MC at weak B

We calculate MC to $O(B^2)$ at weak B. We first compare the various $\Delta G_i^{(j)}$s, with $i, j = {\rm L}, {\rm H}$. We start with the H-state contribution. According to section 4.2, we have

$$\Delta G_{\rm H}^{(\rm H)}(B) \approx -G_0 D_{\rm H}\sum_{n\in\text{H-states}}\sum_{m}^{m_{\max}^{(\rm H)}}\Delta_{n,m}$$

with

$$\Delta_{n,m} \equiv \int_{Q_m}^{Q_{m+1}}\frac{{\rm d}^2\vec{k}_\parallel}{(2\pi)^2}\left\{\frac{p_{n,m}|_{\rm H}}{\lambda_{n,K_m=0}+D_{\rm eff}(n)K_m^2+1/\tau_\phi^{(\rm H)}} - \frac{p_{n,\vec{k}_\parallel=0}|_{\rm H}}{\lambda_{n,K_m=0}+D_{\rm eff}(n)k_\parallel^2+1/\tau_\phi^{(\rm H)}}\right\}.$$

Since $p_{n,m}|_{\rm H} \sim p_{n,\vec{k}_\parallel=0}|_{\rm H}$ for H states, we can factor out the probability and write

$$\Delta G_{\rm H}^{(\rm H)}(B) \approx -G_0 D_{\rm H}\sum_{n\in\text{H-states}}p_{n,K_m=0}|_{\rm H}\sum_{m}^{m_{\max}^{(\rm H)}}\Delta'_{n,m}$$

where

$$\Delta'_{n,m} \equiv \int_{Q_m}^{Q_{m+1}}\frac{{\rm d}^2\vec{k}_\parallel}{(2\pi)^2}\left\{\frac{1}{\lambda_{n,K_m=0}+D_{\rm eff}(n)K_m^2+1/\tau_\phi^{(\rm H)}} - \frac{1}{\lambda_{n,K_m=0}+D_{\rm eff}(n)k_\parallel^2+1/\tau_\phi^{(\rm H)}}\right\}$$

is slightly different from $\Delta_{n,m}$. Likewise, we write

$$\Delta G_{\rm L}^{(\rm H)}(B) \approx -G_0 D_{\rm L}\sum_{n\in H-states}p_{n,K_m=0}|_{\rm L}\sum_{m}^{m_{\max}^{(\rm H)}}\Delta'_{n,m}.$$

Hence, we obtain the ratio

$$\frac{\Delta G_{\rm L}^{(\rm H)}}{\Delta G_{\rm H}^{(\rm H)}} \sim \frac{D_{\rm L}}{D_{\rm H}}\left\langle\frac{p_{n,K_\mu=0}|_{\rm L}}{p_{nK_\mu=0}|_{\rm H}}\right\rangle \leqslant \frac{1}{\beta}\frac{\gamma}{\alpha} < 1 \tag{5.2.1}$$

which is analogous to equation (5.1.1).

On the other hand, for the L-state contribution, we have

$$\Delta G_{\rm L}^{(\rm L)}(B) \approx -G_0 D_{\rm L} \sum_{n\in \text{L-states}} p_{n,K_m=0}|_{\rm L} \sum_{m}^{m_{\max}^{(\rm L)}} \Delta'_{n,m}. \quad (5.2.2)$$

$$\Delta G_{\rm H}^{(\rm L)}(B) \approx -G_0 D_{\rm H} \sum_{n\in \text{L-states}} p_{n,K_m=0}|_{\rm H} \sum_{m}^{m_{\max}^{(\rm L)}} \Delta''_{n,m} \quad (5.2.3)$$

where

$$\Delta''_{n,m} \equiv \int_{Q_m}^{Q_{m+1}} \frac{d^2\vec{k}_\parallel}{(2\pi)^2} \left\{ \frac{f''_{n,K_m}}{\lambda_{n,K_m=0} + D_{\rm eff}(n)K_m^2 + 1/\tau_\phi^{(\rm L)}} - \frac{f''_{n,k_\parallel}}{\lambda_{n,K_m=0} + D_{\rm eff}(n)k_\parallel^2 + 1/\tau_\phi^{(\rm L)}} \right\}.$$

Note that $\Delta G_{\rm H}^{(\rm L)}(B)$ is written in terms of $\Delta''_{n,m}$ which is slightly different from $\Delta'_{n,m}$, with the extra factor f'' being present in $\Delta''_{n,m}$. f'' is closely related to f introduced in equation (3.7*e*) for below-barrier L states. Its definition is given below

$$f''_{n,K_\mu} \equiv \begin{cases} 1, & \text{for above-barrier states} \\ f_{n,\mu}, & \text{for below-barrier states.} \end{cases}$$

The reason for the appearance of f'' is that $\Delta G_{\rm H}^{(\rm L)}(B)$ contains contributions from both below-barrier and above-barrier L states. For above-barrier states, the H-region probability is given as $p_{n,K_\mu}|_{\rm H} \sim p_{n,K_\mu=0}|_{\rm H}$, while for below-barrier L states, it is $p_{n,K_\mu}|_{\rm H} \sim p_{n,K_\mu=0}|_{\rm H} f_{n,m}$, as given in equation (3.7*e*).

With the presence of the factor f'' in $\Delta G_{\rm H}^{(\rm L)}(B)$, it is less trivial to calculate the ratio $\frac{\Delta G_{\rm H}^{(\rm L)}}{\Delta G_{\rm L}^{(\rm L)}}$. It turns out that one still obtains

$$\frac{\Delta G_{\rm H}^{(\rm L)}}{\Delta G_{\rm L}^{(\rm L)}} \leqslant \frac{\gamma}{\alpha\chi^2} < 1, \quad (5.2.4)$$

which is analogous to equation (5.1.2). The proof is a little lengthy and thus is omitted here.

According to equations (5.2.1) and (5.2.4), we can drop $\Delta G_{\rm H}^{(\rm L)}$ and $\Delta G_{\rm L}^{(\rm H)}$ and write $\Delta G \sim \Delta G_{\rm H}^{(\rm H)} + \Delta G_{\rm L}^{(\rm L)}$ within logarithmic accuracy. We evaluate $\Delta G_{\rm H}^{(\rm H)}$ first and then $\Delta G_{\rm L}^{(\rm L)}$.

Calculation of $\Delta G_H^{(H)}$. According to section 4.2

$$\Delta G_{\rm H}^{(\rm H)}(B) \approx \frac{G_0}{24\pi l_B^4} \sum_{n=1}^{N_{\max}^{(\rm H)}} \frac{D_{\rm H}^2}{\left(D_{\rm H}\frac{n^2\pi^2}{H^2} + \tau_\varphi^{(H)-1}\right)^2} = \frac{G_0 H^4}{24\pi^5 l_B^4} F\left(\frac{l_\varphi^{(\rm H)}}{H}; N_{\max}^{(\rm H)}\right) \quad (5.2.5)$$

where $l_\varphi^{(\rm H)} \equiv \sqrt{D_{\rm H}\tau_\varphi^{(\rm H)}}$ and we have taken $p_{n,K_\mu=0}|_{\rm H} \sim 1$, $D_{\rm eff}(n) \sim D_{\rm H}$ and $\lambda_{n,K_\mu=0} \sim D_{\rm H}\frac{n^2\pi^2}{H^2}$, $n = 1, 2, \ldots$ for H states. The function $F(x; N)$ in equation (5.2.5) is defined as

$$F(x; N) \equiv \sum_{n=1}^{N} \frac{1}{\left(n^2 + 1/(\pi x)^2\right)^2},$$

with the property

$$F(x; N) \sim O(1)(\pi x)^3 \qquad \text{for } \pi x < O(1) \quad (\text{i.e., } 1/\tau_\varphi^{(\rm H)} > O(D_{\rm H}/H^2)) \quad (5.2.6a)$$

$$F(x; N) \sim O(1) \qquad \text{for } \pi x > O(1) \quad (\text{i.e. } 1/\tau_\varphi^{(\rm H)} < O(D_{\rm H}/H^2)). \quad (5.2.6b)$$

For the regime $T_{\rm L} < T$, $\Delta G_{\rm L}^{(\rm L)} \sim 0$ and $\Delta G \sim \Delta G_{\rm H}^{(\rm H)}$. Equations (5.2.5) and (5.2.6*a*) show strong $1/\tau_\varphi^{(\rm H)}$ dependence for ΔG at high $1/\tau_\varphi^{(\rm H)} > D_{\rm H}/H^2$ (or $T_{\rm H} < T$), with $\Delta G \propto \tau_\varphi^{(H)3/2}$, in agreement with the qualitative discussion in section 4.1. Moreover, equations (5.2.5) and (5.2.6*b*) give the saturated value

$$\Delta G(\text{saturated}) \sim \Delta G_{\rm H}^{(\rm H)}(\text{saturated}) \sim O(1)\frac{G_0 H^4}{24\pi^5 l_B^4}$$

for $T_{\rm L} < T \leqslant T_{\rm H}$.

Calculation of $\Delta G_L^{(L)}$. We calculate $\Delta G_{\rm L}^{(\rm L)}$ in the regime $T \leqslant T_{\rm L}$. According to section 4.2

$$\Delta G_{\rm L}^{(\rm L)}(B) \approx \frac{G_0}{24\pi l_B^4} \sum_{n=0}^{N_{\max}^{(\rm L)}} \frac{D_{\rm L}^2}{\left(D_{\rm L}\frac{n^2\pi^2}{L^2} + \tau_\varphi^{(L)-1}\right)^2} = \frac{G_0 l_\varphi^{(\rm L)4}}{24\pi^5 l_B^4} + \frac{G_0 L^4}{24\pi^5 l_B^4} F\left(\frac{l_\varphi^{(\rm L)}}{L}; N_{\max}^{(\rm L)}\right) \quad (5.2.7)$$

where $l_\varphi^{(\rm L)} \equiv \sqrt{D_{\rm L}\tau_\varphi^{(\rm L)}}$ and we have taken $p_{n,K_\mu=0}|_{\rm L} \sim 1$, $D_{\rm eff}(n) \sim D_{\rm L}$ and $\lambda_{n,K_\mu=0} \sim D_{\rm L}\frac{n^2\pi^2}{L^2}$, $n = 0, 1, 2, \ldots$ for L states. The function $F(x; N)$ is as defined previously.

The first term in equation (5.2.7) derives from the zero mode (i.e. $n = 0$ L state) in the sum. It varies like $\tau_\varphi^{(\rm L)2}$ and describes the MC of a 2D film. The second term derives from the remaining $n \neq 0$ states. According to the property of $F(x; N)$ listed in (5.2.6*a*) and (5.2.6*b*), it varies like $\tau_\varphi^{(L)3/2}$ for $l_\varphi^{(\rm L)}/L < O(1)$ (or $\frac{1}{\tau_\varphi^{(\rm L)}} > O(\frac{D_{\rm L}}{L^2})$) and becomes saturated for $l_\varphi^{(\rm L)}/L > O(1)$ (or $\frac{1}{\tau_\varphi^{(\rm L)}} < O(\frac{D_{\rm L}}{L^2})$). Thus, the second term describes the MC of an L bulk with a saturated dephasing time $\tau_\varphi^{(\rm L)(\rm eff)} \sim 1/\lambda_{n=1,K_\mu=0} \sim \frac{L^2}{D_{\rm L}}$. The bulk term dominates at high $1/\tau_\varphi^{(\rm L)}$ while the film term does so at low $1/\tau_\varphi^{(\rm L)}$. The crossover from bulk-like to film-like behavior occurs at $T'_{\rm crossover}$, which is determined by

$$\tau_\varphi^{(\rm L)}(T'_{\rm crossover}) \sim \tau_\varphi^{(\rm L)(\rm eff)}, \quad (5.2.8)$$

where the bulk and film terms are comparable.

Total magnetoconductance ΔG. One can combine the results (5.2.5) and (5.2.7) to obtain $\Delta G \sim \Delta G_{\rm H}^{(\rm H)} + \Delta G_{\rm L}^{(\rm L)}$ and verify the overall low-temperature behavior of ΔG discussed in section 4.1. Analogous to the case of δG, the additional contribution of $\Delta G_{\rm L}^{(\rm L)}$ to ΔG for $T \leqslant T_{\rm L}$ generally gives a sharp rise in ΔG. The rise is described by equation (5.2.7), firstly being bulk-like and varying as $\tau_\varphi^{(\rm L)3/2}$, and then crossing over to being film-like at $T'_{\rm crossover}$. Beyond the crossover, ΔG

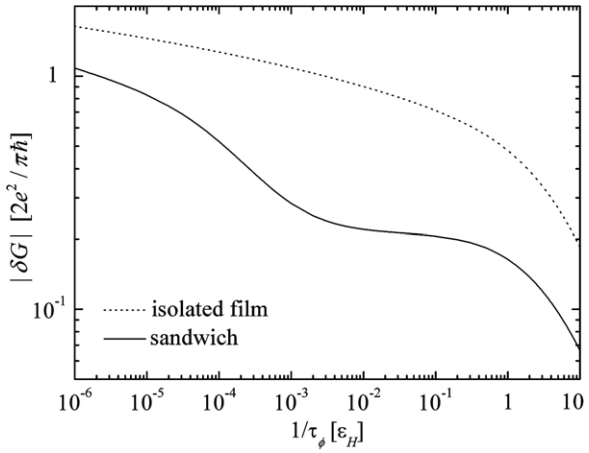

Figure 4. $|\delta G|$ (in units of $2e^2/\pi\hbar$) versus $1/\tau_\phi$ (in units of $\varepsilon_{\rm H} \equiv D_{\rm H}(\pi/H)^2$) for the sandwich structure and the isolated film. We take $L = H/2, \alpha = 10, \beta = 4000, \gamma = 2$. Dashed curve—isolated film; solid curve—sandwich structure.

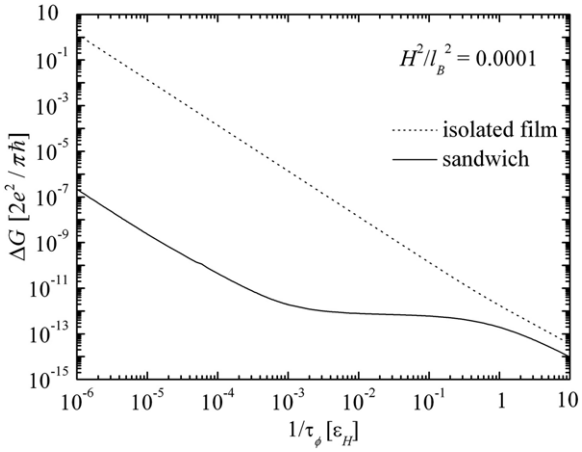

Figure 5. MC (in units of $2e^2/\pi\hbar$) versus $1/\tau_\phi$ (in units of $\varepsilon_{\rm H} \equiv D_{\rm H}(\pi/H)^2$) for the sandwich structure and the isolated film. The parameters used are the same as those in figure 4. The applied magnetic field is specified by the value $H^2/l_B^2 = 0.0001$.

diverges as $\tau_\varphi^{({\rm L})2}$ until the size effect sets in at the temperature where $\tau_\varphi^{({\rm L})} \sim \tau_{yz}^{({\rm c})}$. However, things are different in the limit of a clean L bulk where $l_{\rm L} \sim L \sim L_{yz}$. In this case, we have $\tau_{\rm L} \sim \tau_{yz}^{({\rm c})}$. This shuts off the window $\tau_{\rm L} < \tau_\varphi^{({\rm L})} < \tau_{yz}^{({\rm c})}$ in which backscattering interference in the L region is allowed to happen. Therefore, backscattering hardly occurs and $\Delta G_{\rm L}^{({\rm L})}$ is nearly zero (equation (5.2.7) for $\Delta G_{\rm L}^{({\rm L})}$ does not apply here). Thus, the total MC saturates at $\Delta G \sim \Delta G_{\rm H}^{({\rm H})}$(saturated) for $T \leqslant T_{\rm L}$ down to 0 K.

6. Film-like sandwich structure versus isolated H film (numerical results)

In this section, we calculate numerically all $\delta G_i^{(j)}$s and $\Delta G_i^{(j)}$s, with the formulae presented in section 4.2, and combine them to obtain the total δG and MC. Parameters of the structure in the calculation are specified as follows. In general, $1/\tau_\varphi^{({\rm H})}(T)$ and $1/\tau_\varphi^{({\rm L})}(T)$ are material- and structure-dependent. For clarity of presentation, we shall take $1/\tau_\varphi^{({\rm H})} = 1/\tau_\varphi^{({\rm L})}$ and denote both as $1/\tau_\varphi$. With this assumption, (SAT′) in section 4.1 reduces to

$$\gamma^2/\beta\chi^2 < 1.$$

It shows that saturation may occur with either film-like structures (with $\beta \gg 1$) or bulk-like structures (with $\chi \gg 1$). For a demonstration, we focus on a film-like structure. A brief discussion about bulk-like structures is given at the end of this section. The film-like sandwich structure considered has parameters $L = H/2, \alpha = 10, \gamma = 2$ and its behavior is compared to that of an isolated H film with thickness $= H, \alpha = 10$. The parameter β is varied and specified in each case.

The conductance correction is shown in figure 4 and MC is shown in figure 5. $\beta = 4000$ is used in both cases. In the figures, the characteristic inverse times are $\varepsilon_{\rm H} \equiv D_{\rm H}(\pi/H)^2$ and $1/\tau_{\rm L}[\sim \frac{\gamma^2}{\beta\chi^2}\varepsilon_{\rm H}]$. Firstly, the result of a sandwich structure

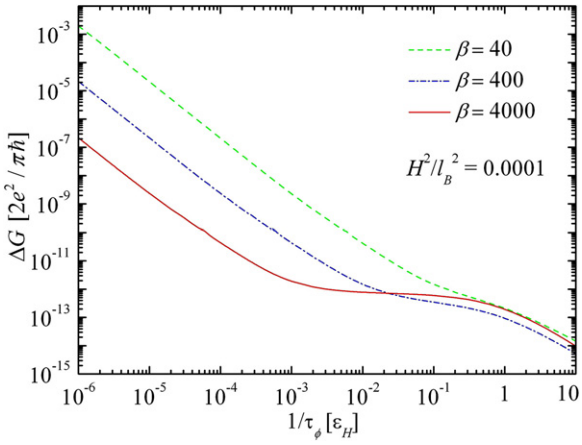

Figure 6. MC (in units of $2e^2/\pi\hbar$) versus $1/\tau_\phi$ (in units of $\varepsilon_{\rm H} \equiv D_{\rm H}(\pi/H)^2$) for the sandwich structure. Parameters, except for β, are the same as those taken in figure 4. Three values of β are used—$\beta = 40$ (dashed curve), $\beta = 400$ (dashed–dotted curve) and $\beta = 4000$ (solid curve). The applied magnetic field is specified by the value $H^2/l_B^2 = 0.0001$.

is reduced relative to that of the film over the whole range of $1/\tau_\varphi$ shown in the graph, in both figures. In fact, this relative reduction constantly shows up also with other values of β (see figure 6 for data with $\beta = 40$ and 400), and may be regarded as the precursor of saturation regardless of whether a good look of saturation actually appears. Secondly, at the low-temperature side (i.e. $1/\tau_\varphi < \varepsilon_{\rm H}$), both δG and MC for the isolated film increase with decreasing $1/\tau_\varphi$, as is typical with an ideal Q2D system. But for the sandwich structure, they remain nearly constant for $1/\tau_{\rm L} < 1/\tau_\varphi \leqslant \varepsilon_{\rm H}$. It shows that the sandwich structure behaves like the film with effectively a finite phase breaking time $\tau_\varphi^{({\rm eff})} \sim O(1/\varepsilon_{\rm H})$, even when the true rate is reduced to low $1/\tau_\varphi < O(\varepsilon_{\rm H})$. However, both δG and MC eventually increase sharply at extremely low $1/\tau_\varphi \leqslant 1/\tau_{\rm L}$. Last, perhaps not surprisingly, results for the two structures (i.e. sandwich and film) appear to converge at high

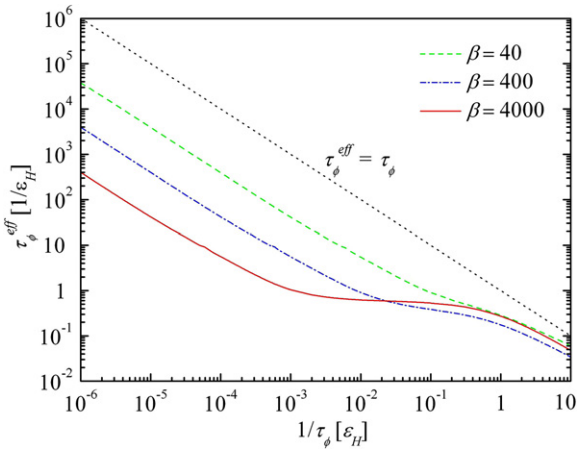

Figure 7. $\tau_\varphi^{(\mathrm{eff})}$ (in units of $1/\varepsilon_\mathrm{H} \equiv (H/\pi)^2/D_\mathrm{H}$) versus $1/\tau_\varphi$ (in units of $\varepsilon_\mathrm{H} \equiv D_\mathrm{H}(\pi/H)^2$). Parameters, except for β, are the same as those taken in figure 4. Three values of β are used—$\beta = 40$ (dashed curve), $\beta = 400$ (dashed–dotted curve) and $\beta = 4000$ (solid curve).

temperatures (i.e. $1/\tau_\varphi > \varepsilon_\mathrm{H}$), for the following simple reason. With short τ_φ, the phase coherence length $l_\varphi^{(\mathrm{H})}$ is smaller than H. It means that, for the sandwich structure, electrons of the conducting channel stay largely in the H region during the backscattering period τ_φ. Such a situation is not much different from that of the isolated film. It thus explains the convergence.

In figure 6, we plot the MC of the sandwich structure for $\beta = 40$, 400 and 4000. It shows the interesting trend that the saturation of MC becomes prominent with increasing β. Because β is the parameter controlling the ratios of transport properties of the H and L regions, it means that the more contrast between the regions, the better the saturation appears.

Comparison of the sandwich structure with an isolated film can also be approached from the following viewpoint. We define the effective dephasing time $\tau_\varphi^{(\mathrm{eff})}$ by requiring

$$\Delta G^{(\mathrm{sandwich})}(\tau_\varphi) = \Delta G^{(\mathrm{film})}(\tau_\varphi^{(\mathrm{eff})}),$$

which means that the orthodox theory of an isolated film is imposed on the MC of a sandwich structure. This determines the function $\tau_\varphi^{(\mathrm{eff})}(1/\tau_\varphi)$ plotted in figure 7 for $\beta = 40$, 400 and 4000. Firstly, it shows that the nominal dephasing time ($\tau_\varphi^{(\mathrm{eff})}$) is suppressed relative to the true one (τ_φ). Secondly, it shows that, with increasing β, $\tau_\varphi^{(\mathrm{eff})}$ begins to show saturation and the look of saturation improves with increasing β. Specifically, the phenomenon of saturation shows clearly for $\beta = 4000$, while for $\beta = 40$, it can hardly be discerned. Last, at extremely low $1/\tau_\varphi \leqslant 1/\tau_\mathrm{L}$, $\tau_\varphi^{(\mathrm{eff})}$ increases sharply in all cases.

Saturation and parameters/structures

In summary, the numerical result has demonstrated clearly that, for film-like structures, the look of saturation improves with increasing β. The trend can also be understood in terms of the condition (SAT′), which shows that (SAT′) is likely to be satisfied with large β in the case of film-like structures. In the following, we briefly discuss the parametric condition for the occurrence of saturation in the case of bulk-like structures. Based on (SAT′), saturation may also occur with $\beta \gg 1$ or, alternatively, with $\chi/\gamma \gg 1$. We make two notes below on the second condition. Firstly, since $\chi/\gamma = l_\mathrm{L}/H$, the condition $\chi/\gamma \gg 1$ leads to $l_\mathrm{L} \gg l_\mathrm{H}$. It means that a relatively clean L region in the structure aids the occurrence of saturation. Secondly, since $L > l_\mathrm{L}$ is required in our work, we further have the condition $L(> l_\mathrm{L}) \gg l_\mathrm{H}$. This puts a constraint on the minimum thickness of the L region and, as such, the condition $\chi/\gamma \gg 1$ is less likely to hold for film-like structures.

7. Remark, summary and conclusion

In this section, we shall summarize the present work. A simple physical picture for dephasing is also offered in terms of electron lifetime in the H layer. A brief discussion guided by the present theory is given for dephasing experiments, where a theoretical estimate of dephasing time is compared with the experimental value. Limitations and future extension of the present theory are discussed.

We have presented a theoretical study of transport properties for a sandwich structure in the weak localization regime. We have considered two classes of structures, namely film-like and bulk-like ones, and have derived analytical estimates of δG and MC applicable to both cases. In general, it shows that, for a certain range of parameters where the condition (SAT) is satisfied, δG and MC may stay nearly constant over a range of temperatures, as if the phase breaking time were saturated.

We have specifically carried out numerical calculations for a film-like structure and compared them with those of a freestanding film. The result confirms the discussion based on analytical estimations. Moreover, it is found that both δG and MC are suppressed with respect to those of the film. It also shows that the better the current is confined (to the H layer by increasing β), the more discernible the saturation becomes. We have also examined the saturation from an alternative viewpoint, with a nominal phase breaking rate defined for a sandwich structure in terms of film theory. We have shown that, while the true phase breaking rate varies, the nominal rate (i.e. $1/\tau_\varphi^{(\mathrm{eff})}$) may stay nearly constant over a range of temperatures.

The saturation demonstrated can intuitively be explained in terms of the characteristics of a sandwich structure. It has the feature that the frequency of backscattering varies dramatically over regions. When the H layer and L regions are in strong contrast, backscattering occurs primarily in the H layer for $T_\mathrm{L} < T$. Once an electron enters the L region, it makes hardly any backscattering, and from that viewpoint it looks as if the electron had decayed, with a lifetime given by $O(H^2/D_\mathrm{H})$, i.e. the time it takes to diffuse out of the H layer. This determines the saturation value of the nominal phase breaking time, with $\tau_\varphi^{(\mathrm{eff})}(\mathrm{saturated}) \sim O(H^2/D_\mathrm{H})$, while the true one varies with T.

As the work shows, at extremely low temperatures where $T \leqslant T_\mathrm{L}$, δG MC, and $\tau_\varphi^{(\mathrm{eff})}$ all diverge for a film-like structure. This is consistent with the experimental observation with $Cu_{93}Ge_4Au_3$ films, reported in [8], of a sharp upturn in MC at the end of saturation. Hopefully, the calculation presented here is relevant to the understanding of such experiments. For

bulk-like structures in the regime $T \leqslant T_{\mathrm{L}}$, δG saturates but MC diverges except in the limit of the clean L bulk.

We also remark on the limitation/future extension of the present theory. Firstly, it is worthwhile to refine the theory. In a moment, we shall compare the present theory with experiments and suggest the direction of improvement for a better agreement with experiments. Secondly, it would be interesting to extend the present theory to different dimensions, e.g. the case of Q1D systems. Thirdly, it would be useful to develop an analogous theory for quantum-confined Q2D systems. Derivation of the present theory is based on the condition that $H > l_{\mathrm{H}} > \lambda_{\mathrm{H}}$ and $L > l_{\mathrm{L}} > \lambda_{\mathrm{L}}$, which is true only in diffusion-confined structures. In the case of quantum-confined Q2D systems, such a condition does not hold and thus the present derivation does not apply. A rigorous derivation of the theory for such systems shall be useful for the experiments with these systems. In the absence of such a derivation, however, in the following we shall rely on the present theory as a guide to discuss dephasing experiments, where quantum-confined systems are as likely to be involved as diffusion-confined ones.

With the above limitation of our theory in mind, we now analyze the experiments of Lin and Giordano with Au–Pd films [6] from the viewpoint of our theory. Two samples are considered. The first sample is characterized by the parameters $D_{\mathrm{H}} = 2.3 \times 10^{-3}$ m^2 s^{-1} and $H = 120$ A. We estimate the saturated value with the formula $\tau_\varphi^{(\mathrm{eff})}(\mathrm{theo.}) \sim H^2/D_{\mathrm{H}}$ which appeared earlier in the qualitative analysis of section 4.1 for diffusion-confined systems, and obtain $\tau_\varphi^{(\mathrm{eff})}(\mathrm{theo.}) \sim 0.63 \times 10^{-13}$ s. In contrast, the experimental value is $\tau_\varphi^{(\mathrm{eff})}(\exp t.) = 6.55 \times 10^{-13}$ s, which is about ten times as large. The second sample is characterized by the parameters $D_{\mathrm{H}} = 0.4 \times 10^{-3}$ m^2 s^{-1} and $H = 160$ A. We estimate the saturated value again with the formula suitable for diffusion-confined structures, and obtain $\tau_\varphi^{(\mathrm{eff})}(\mathrm{theo.}) \sim 6.4 \times 10^{-13}$ s. The experimental value is $\tau_\varphi^{(\mathrm{eff})}(\exp t.) = 1.2 \times 10^{-11}$ s, which is about twenty times as large. Thus, in both cases, $\tau_\varphi^{(\mathrm{eff})}(\exp t.)$ is larger than $\tau_\varphi^{(\mathrm{eff})}(\mathrm{theo.})$ by an order of magnitude.

We propose two different scenarios for the source of the numerical difference between $\tau_\varphi^{(\mathrm{eff})}(\exp t.)$ and $\tau_\varphi^{(\mathrm{eff})}(\mathrm{theo.})$. (A) The samples may be quantum-confined systems, which should, rigorously speaking, be treated with some extended form of the present theory to account for the quantum-mechanical nature of electron movement. (B) Alternatively, the samples may be diffusion-confined, but our estimation within the present (diffusion-confined) model may be oversimplified. For example, it uses the formula suitable for a symmetric I–L–H–L–I sandwich structure while the samples, as non-freestanding films, may be close to asymmetric I–L–H structures (as discussed in section 2). Although the formula should be qualitatively correct also for asymmetric structures, it may result in some numerical difference. Moreover, various parameters, such as L, β, etc, are unknown. Thus, the estimation can only be based on the rough formula given in the qualitative discussion of section 4.1. This may further bring in some differences. Finally, it is important to note that our present classical diffusive theory does not account for the effect of quantum mechanics on the diffusive movement of electrons across the L/H interface. As explained in the following, this quantum effect in fact enhances the dephasing time. According to quantum mechanics, there is a strong reflection of electrons at the L/H interface, with the reflection coefficient estimated by Refl. $= [(\lambda_{\mathrm{H}}/\lambda_{\mathrm{L}} - 1)/(\lambda_{\mathrm{H}}/\lambda_{\mathrm{L}} + 1)]^2 \sim 1 - 2\lambda_{\mathrm{H}}/\lambda_{\mathrm{L}}$ in the limit $\lambda_{\mathrm{L}} \gg \lambda_{\mathrm{H}}$. In a classical theory such as the present one, the interface reflection is completely neglected, and hence the electron lifetime for dwelling in the H layer is the same as the diffusion time $O(H^2/D_{\mathrm{H}})$ (within which an H-layer electron diffuses out of the layer). However, with the reflection taken into account, the H-layer electron undergoes the process of diffusing in the layer and then bouncing back at the L/H interface, for several times, before eventually getting out. Thus, the H-layer dwelling time (which is also the saturated dephasing time, as discussed earlier in this section) is enhanced by the quantum effect. According to the above simple-minded picture, it gives $O(\lambda_{\mathrm{L}}/\lambda_{\mathrm{H}})(H^2/D_{\mathrm{H}})$ as the enhanced dephasing time. In order to match the theoretical values with experimental ones, the foregoing expression of enhanced dephasing would place the enhancement factor $\lambda_{\mathrm{L}}/\lambda_{\mathrm{H}}$ at approximately 10 and 20, respectively, for the two samples. Now, if we take these values and stretch this line of discussion further, an interesting inference may be made, as follows. We begin by noting that, although the two samples differ much in the dephasing time (which can be either theoretical or experimental), the enhancement factor $\lambda_{\mathrm{L}}/\lambda_{\mathrm{H}}$ for the time varies only by a factor of two according to the above estimation. With λ_{H} being already fixed at the typical Fermi wavelength of Au–Pd, it follows that the variation of λ_{L} must be rather insignificant for the samples. Since the value of λ_{L} is determined by the composition and structure of the L layer, one would further infer that, with respect to the samples, the properties of the L layer (or, equivalently, the I/H interface as discussed in section 2) must remain fairly constant. Interestingly, such an inference is actually consistent with the empirical fact that samples grown in the same experimental group tend to have similar interfaces. Thereby, the above discussion of quantum effect shows some physical sense, and it points to the possibility of improving the numerical difference with the inclusion of the quantum effect in the model. However, we note that, although the discussion is made within scenario B and thus lends support to the scenario, it is not conclusive enough to rule out scenario A.

Last, the above numerical comparison shows that, in order to analyze the current dephasing experiments more accurately, it is imperative to extend the theory and incorporate the quantum-mechanical nature of electron motion, regardless of the type of systems involved. We hope to see such a development in the future.

Acknowledgment

We acknowledge the support of the National Science Council in the ROC through contract no. 96-2112-M-007-029.

References

[1] Abrahams E, Anderson P W, Licciardello D C and Ramakrishnan T V 1979 *Phys. Rev. Lett.* **42** 673

[2] For a good theoretical review, see, for example: Altshuler B L, Aronov A G, Khmelnitskii D E and Larkin A I 1982 *Quantum Theory of Solids* ed I M Lifshits (Moscow: Mir)

[3] Altshuler B L, Aronov A G and Khmelnitskii D E 1982 *J. Phys. C: Solid State Phys.* **15** 7367

[4] Bergmann G 1984 *Phys. Rep.* **107** 1 and references therein

[5] Mohanty P, Jariwala E M Q and Webb R A 1997 *Phys. Rev. Lett.* **78** 3366
Mohanty P and Webb R A 2002 *Phys. Rev. Lett.* **88** 146601

[6] Lin J J and Girodano N 1987 *Phys. Rev.* B **35** 1071
Pooke D M, Paquin N, Pepper M and Gundlach A 1989 *J. Phys.: Condens. Matter* **1** 3289
Hiramoto T *et al* 1989 *Appl. Phys. Lett.* **54** 2103
Mueller R M, Stasch R and Bergmann G 1994 *Solid State Commun.* **91** 255

[7] Pierre F and Birge N O 2002 *Phys. Rev. Lett.* **89** 206804

[8] Huang S M, Lee T C, Akimoto H, Kono K and Lin J-J 2007 *Phys. Rev. Lett.* **99** 046601

[9] Golubev D S and Zaikin A D 1998 *Phys. Rev. Lett.* **81** 1074

[10] Zawadowski A, von Delft J and Ralph D C 1999 *Phys. Rev. Lett.* **83** 2632

[11] Marquardt F, von Delft J, Smith R A and Ambegaokar V 2007 *Phys. Rev.* B **76** 195331
von Delft J, Marquardt F, Smith R A and Ambegaokar V 2007 *Phys. Rev.* B **76** 195332

[12] Germanenko A V, Minkov G M and Rut O E 2001 *Phys. Rev.* B **64** 165404

[13] *Taurus Medici User's Guide* 2006 (Mountain View, CA: Synopsys)

[14] Lifshitz E M and Pitaevskii L P 1995 *Physical Kinetics* (Woburn, MA: Butterworth-Heinemann)